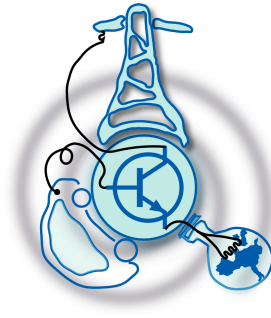


Electric Power Systems Security Analysis in Smart Grids with Renewable Energy

by
José Pablo Figueroa Zelaya



Submitted to the Department of Electrical Engineering, Electronics,
Computers and Systems
in partial fulfillment of the requirements for the degree of
Erasmus Mundus Master Course in Sustainable Transportation and
Electrical Power Systems

at the
UNIVERSIDAD DE OVIEDO

September 2017

© Universidad de Oviedo 2017. All rights reserved.

Author

Certified by

Rui Pestana
External Institution Advisor
Thesis Supervisor

Certified by

Cristina Agreira
STEPS Consortium Advisor
Thesis Supervisor

Electric Power Systems Security Analysis in Smart Grids with Renewable Energy

by

José Pablo Figueroa Zelaya

Submitted to the Department of Electrical Engineering, Electronics, Computers and
Systems

on September 06, 2017, in partial fulfillment of the
requirements for the degree of

Erasmus Mundus Master Course in Sustainable Transportation and Electrical
Power Systems

Abstract

With the current increase of penetration of distributed energy sources (DES), distribution network operators (DSOs) face new challenges in achieving reliable operation of their networks. One of these challenges is uncontrolled islanding. Uncontrolled live islands may occur when an outage part of a network has online generation for which the DSO has no real-time control or previously established management protocol. In the presence of this issue, the DSO would be forced to implement tight frequency and voltage range in their protection schemes that do are not necessarily compatible with European Network Codes. The purpose of this study is to identify live islands that occur in distribution networks in case of line outages due to contingencies or other reasons. Once live islands are identified, their feasibility is determined by performing a nodal power assessment and calculating for power mismatch, frequency stability and voltage stability. An assessment is made for the best course of action to achieve appropriate conditions for either reconnecting the island or perform a controlled shut-down. This course of action can be complementary steps taken on the demand side (demand response) or generation side (generation response). Previously established protocols along with enhanced communication between the network and the dispatch center will ultimately lead to efficient asset management and improved reliability for the customer.

Keywords: distributed energy sources, islanding, demand response, generation response, voltage stability, frequency stability

Thesis Supervisor: Rui Pestana

Title: External Institution Advisor

Thesis Supervisor: Cristina Agreira

Title: STEPS Consortium Advisor

Acknowledgements

This thesis represents an end of a journey that has taken me through several countries, many cities and a myriad of experiences. Thanks a lot to the STEPS Consortium for granting me the opportunity to learn from several great universities where great people learn and work. The STEPS program is an amazing experience and I can rest assured that, in the words of Dave Matthews, I made “The Best of What’s Around.”

I want to thank Rui Pestana, my thesis main advisor. From the moment I arrived to Lisbon, he was extremely helpful, patient, kind and always available to sort out any issues that may have risen along the way. To these amazing qualities, he adds a rarely seen and exceptional professionalism and expertise to his work, from which I was able to learn a great deal. Thank you Rui.

I also want to thank Cristina Agreira, my thesis co-advisor. Cristina was always available whenever I needed some help and made sure that my experience during my internship was as gratifying as possible.

Thanks to my colleagues at R&D NESTER for giving me such a warm welcome to your company. You included me as one more in your lunches, conversations and activities and I am very happy to have met you all.

Thanks to all of my friends and family. My grandfather used to say that having friends is better than having money in the bank. I am still too young to judge the words of wise men, but if what he said is true, I am very rich. Thanks for all of your acts of support, from the smallest one to the grandest ones. You know who you are, and I will make sure to thank each one of you personally. A special thanks to my brothers, who remind me “we’ll always have each other, when everything else is gone.”

Finally, abiding by some ancient law of an old Book, honor must be given to Odalys Zelaya and José Abelardo Figueroa. They are strong, loving, courageous, supporting and kickstarters of an adventure called life. They are mom and dad. Parents are like one’s own personal museum. Reminders of who you used to be, inspiration of what you can be. Thanks mom, thanks dad.

Contents

Contents	iii
List of Figures	v
List of Tables	vii
List of Acronyms	viii
List of Symbols	x
1 Introduction	1
1.1 Work Description and Objectives	1
1.2 State of the art	3
1.2.1 Distributed Energy Sources in Distribution Networks	3
1.2.2 Challenges in Island Operation	4
1.2.3 Dynamic Security Assessments	5
2 Island Identification	8
2.1 Description of Algarve Distribution Network	8
2.2 Islanding Detection Techniques	11
2.3 Proposed Topological Algorithm	13
2.4 Python Script	14
2.5 Results	15
2.5.1 Topology Analysis Results before N-1 and N-2 Contingency Cases	15
2.5.2 Topology Analysis Results for N-1 and N-2 Contingency Cases	15

3	Voltage Security Assessment	18
3.1	Definition	18
3.2	Mathematical Derivation of PV and QV Curves	20
3.3	PV Curves	22
3.4	QV Curves	23
3.5	Results of PV and QV Curves	25
3.5.1	Porto de Lagos Island PV and QV Results	25
3.5.2	Vila do Bispo Island PV and QV Results	25
4	Frequency Security Assessment	28
4.1	Model Description	29
4.2	Inertial Response	31
4.3	Load Self-Regulation	33
4.4	Under Frequency Load Shedding	33
4.5	Synthetic Inertia	35
4.6	Excel/VBA Tool	39
4.7	FSA Results	44
4.7.1	Scenario 1	45
4.7.2	Scenario 2	47
4.7.3	Scenario 3	49
5	Conclusions, Recommendations and Future Work	51
5.1	Conclusions	51
5.2	Recommendations	53
5.3	Future Work	54
A	VBA code	55
B	Quality Report	60
	Bibliography	61

List of Figures

1-1	Distribution network in Algarve, showing HV/MV substations and the corresponding MV network	2
1-2	Typical workflow for DSA	6
1-3	Dynamic phenomena in different timeframes	7
2-1	Distribution network in Algarve, showing TN substations and 60 kV DN substations	9
2-2	Voltage VS	12
2-3	BFS order of node traversing	13
2-4	Python script workflow	14
2-5	Geographic location of islands studied in this work	17
2-6	Network location of islands studied in this work	17
3-1	Single line representation of single-load, infinite-bus system	20
3-2	PV curve	23
3-3	QV curve	24
3-4	Porto de Lagos island PV curve	26
3-5	Porto de Lagos island QV curve	26
3-6	Vila do Bispo island PV curve	27
3-7	Vila do Bispo island QV curve	27
4-1	Block diagram of single busbar model	30
4-2	Response time of frequency-related mechanisms and reactions	31
4-3	Typical WTG Type 1 configuration	36

4-4	Typical WTG Type 2 configuration	36
4-5	Typical WTG Type 3 configuration	37
4-6	Typical WTG Type 4 configuration	37
4-7	Typical WTG Type 5 configuration	38
4-8	Parameters sheet of Excel tool	39
4-9	Generators sheet of Excel tool	40
4-10	UFLS sheet of Excel tool	41
4-11	VBA code flowchart	43
4-12	Output sheet of Excel tool after VBA code is run	43
4-13	Output plot for Porto de Lagos island, Scenario 1	46
4-14	Output plot for Vila do Bispo island, Scenario 1	46
4-15	Output plot for Porto de Lagos island, Scenario 2	48
4-16	Output plot for Vila do Bispo island, Scenario 2	48
4-17	Output plot for Porto de Lagos island, Scenario 3	50
4-18	Output plot for Vila do Bispo island, Scenario 3	50

List of Tables

2.1	Distributed generation in Algarve	9
2.2	Distribution network substations and associated transmission network substations	10
2.3	Network islands studied in Algarve	16
3.1	Active and reactive power security margins	27
4.1	Existing UFLS scheme in Portimão substation	34
4.2	Proposed UFLS scheme	35

List of Acronyms

AC	Alternating Current
BFS	Breadth-First Search
CSV	Comma-Separated Values
DES	Distributed Energy Sources
DFS	Depth-First Search
DN	Distribution Network
DSA	Dynamic Security Assessment
DSO	Distribution System Operator
ENTSO-E	European Network of Transmission System Operators for Electricity
FSA	Frequency Security Assessment
GPS	Global Positioning System
HV	High Voltage
LFSM-O	Limited Frequency System Mode for Over-frequency
MV	Medium Voltage
NDZ	Non-Detection Zones
NEW	This is NEW
OVF/UVF	Over/Under Frequency Protection
OVP/UVF	Over/Under Voltage Protection
PMU	Phasor Measurement Unit
PRC	Primary Reserve Control
PSS/E	Power System Simulator for Engineering
RES	Renewable Energy Sources

RfG	Requirements for Grid connection
ROCOF	Rate Of Change Of Frequency
SCADA	Supervisory Control And Data Acquisition
SRC	Secondary Reserve Control
TN	Transmission Network
TSO	Transmission System Operator
UFLS	Under-Frequency Load Shedding
VBA	Visual Basic for Applications
VS	Vector Surge
VSA	Voltage Security Assessment
WTG	Wind Turbine Generator

List of Symbols

E	generator voltage	[V]
G	nominal power	[W]
H	acceleration time constant	[s]
I	line current	[A]
I	moment of inertia	[kg-m ²]
K_r	self-regulation coefficient	[W/Hz]
P	active power	[W]
Q	reactive power	[VAR]
S	apparent power	[VA]
T	torque	[N-m]
V	bus voltage	[V]
W_k	kinetic energy	[J]
X	reactance	[Ω]
ω_m	angular velocity	[rad-s ⁻¹]
θ_m	angular displacement	[rad]
θ	phase angle	[rad]
f	frequency	[Hz]

Chapter 1

Introduction

1.1 Work Description and Objectives

As distributed energy sources (DES) penetration is high in Portugal with large amounts of geographically dispersed wind farms and increasing number of other generation from RES connected to the distribution network, uncontrolled islanding and weak grid support is a current issue that is being studied and prepared for by the transmission system operator (TSO), which is the company REN, and by the distribution system operator (DSO), which is the company EDP.

The purpose of this work is to identify live islands that may occur in a given distribution network in case of contingencies or other reasons. The distribution network studied is in the region of Algarve, south of Portugal, seen in Figure 1-1. Once live islands are identified, their feasibility is determined by power mismatch criteria and performing a frequency security assessment (FSA) and a voltage security assessment (VSA). FSA is done using a single busbar model and relevant control reactions and VSA is done using information obtained from PV and QV curves. In the scope of this work, the identified islands have asynchronous generation, which makes the study of angle stability not relevant as this concerns the difference in rotor angle between synchronous generators in a coherent group.

The main objective is to assess if previously established protocols along with offline studies can make the operational case of installing enhanced communication

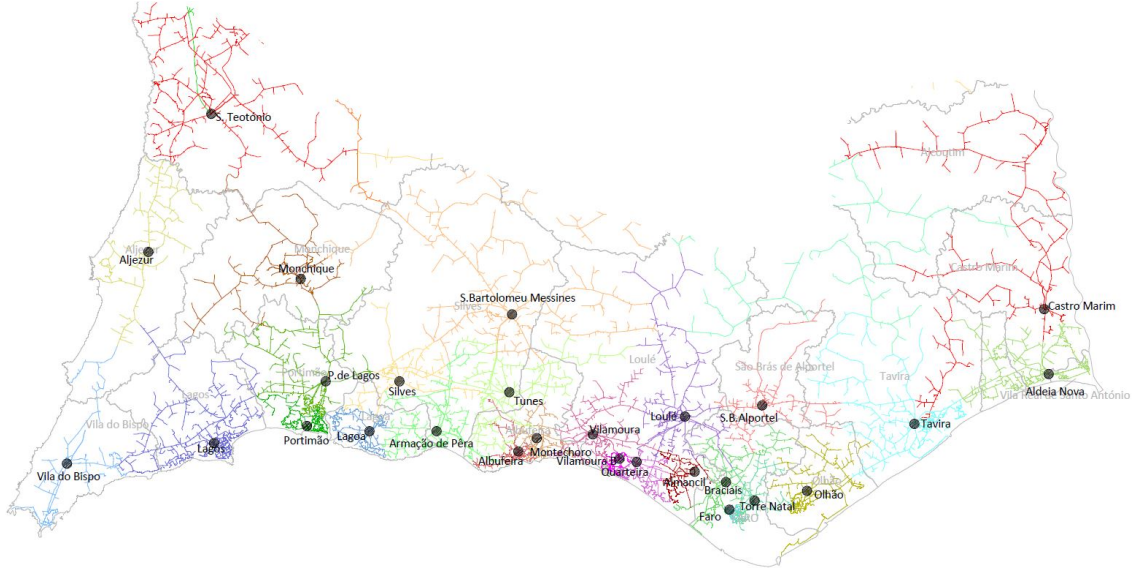


Figure 1-1: Distribution network in Algarve, showing HV/MV substations and the corresponding MV network [1]

between the network and the dispatch center that can ultimately lead to efficient asset management and improved reliability for the customer. Conclusions are made regarding the results of the study and recommendations are stated for the possible courses of action to achieve secure operation of the system.

The report will therefore have the following main chapters:

1. **Introduction**
2. **Island Identification**
3. **Voltage Security Assessment**
4. **Frequency Security Assessment**
5. **Conclusions, Recommendations and Future Work**

The present chapter of “Introduction” introduces the topics studied in this work and state the final scope and objectives. The chapter of “Island identification” proceeds with description of existing methodologies for island identification and the proposed methods used for this work to identify island candidates. “Voltage security assessment” and “Frequency security assessment” chapters describe the methods chosen

to assess for system secure operation, the tools used and developed for these methods and the results of the assessments. Finally, the “Conclusions” chapter summarizes the facts learned during this work and make some recommendations for enhanced system operation and future follow-up work of what has already been started.

This report is presented as fulfillment of final thesis work and internship of the Erasmus Mundus Master Course on Sustainable Transportation and Electrical Power Systems (EMMC STEPS). The work was done during a five months internship in R&D NESTER. R&D NESTER is a research and development company owned by the REN Group and by the State Grid Corporation of China.

1.2 State of the art

1.2.1 Distributed Energy Sources in Distribution Networks

With the current increasing penetration of DES in the distribution networks, the paradigm of centralized electricity production supplying a centralized demand is changing. Nowadays generation, especially from renewable energy sources (RES), is being installed in more dispersed locations following either load or energy source conditions. The distributed nature of this generation brings about new challenges in its design, control and assessment. The trend of work towards smarter grids demands for new engineering approaches using either common or novel techniques.

Both TSOs and DSOs have had different issues when dealing with DES. While TSOs previously used to have more control over centralized generating units with DSOs dealing only with the distribution of electricity to clients, nowadays roles are changing. Even though TSOs continue to have control and responsibility over the transmission network and centralized generating units, they lose their share of control over the total generating capacity as new units are being installed in the distribution level. This increases the uncertainty when performing security assessments over assets that are not fully accounted for. Meanwhile DSOs have had their share of control and responsibility over generating capacity increased. The two main DES are wind and

solar energy, and their generating units are mainly installed in geographic locations favoring the extraction of energy. In many cases they are installed in the same locations as load centers, as can be seen often with solar panels being installed in buildings' rooftops. This new scenario may place DSOs in a position where they should meet operating criteria that was previously determined for TSOs.

Problems may arise when interfacing with the transmission network where issues such as system security and grid support are considered. The European network code (RfG) defines the limits for maximum capacity for generator types in Continental Europe as 0.8 kW or more for type A, 1 MW for type B, 50 MW for type C and 75 MW for type D [2]. Regarding frequency operating criteria, RfG defines a frequency range of 47.5 Hz to 51.5 Hz for all generators types A, B, C and D connected to the grid. These criteria encompass a lot of generating modules that are connected to the distribution network. Having generating modules connected to the grid and operating in a wide frequency range allows for frequency support and control in the event of contingencies. Nowadays an important number of generating capacity located in the distribution network operates in a shorter frequency range. The European Network of Transmission System Operators for Electricity (ENTSO-E) has determined that an important quantity of the total generating capacity in Europe can be lost at some specific frequency thresholds, which jeopardizes the security of the overall system [3].

1.2.2 Challenges in Island Operation

One of the challenges of DES is the frequency operating range of generating units. Frequency operating range of generating units in the distribution network tends to be stricter than the range stated in the RfG. The strict ranges are suitable for their goals of protecting the machines from operating in dangerous conditions, and therefore protecting the human personnel working near the machines. This protection considers generating units that provide little or no inertia to the system, which would force the machines to abruptly disconnect in the event of minor contingencies, causing unnecessary stress in all the associated equipment. Another reason for having strict operating ranges is to avoid the creation of uncontrolled live islanding when facing

contingencies. Island operation is defined in the RfG as an isolated part of the network with at least one generating module controlling frequency and voltage. The problem is when island operation is not previously envisioned for such part of the network, frequency and voltages are not controlled and protection schemes are installed to promptly detect the islanding and eliminate it before conditions worsen. Without appropriate sensors or information from security assessments, these measures and strict operating conditions could be widely found in the distribution network. To mitigate the problem, several courses of actions can be implemented, which have already been mentioned by ENTSO-E in several studies.

Online island detection is often made by measuring frequency deviations [3], but these measurements are often not reliable [4]. Another alternative is massive installation of phasor measurement units (PMUs) which provide a very accurate measurement of phasor, frequency and ROCOF synchronized in a time frame usually obtained from GPS signals [5]. These units are currently quite expensive to install in a distribution network in large enough numbers to provide wide coverage.

A different method proposed and used in this work for island detection is an offline topological assessment of the system. This assessment coupled with enhanced communication in the distribution network and generation and load information can identify possible occurring islands for different scenarios. That information can be used in a rollout plan of enhanced sensors and communication devices within the distribution network, installing the appropriate devices in elements of the system identified in the offline study as prone to creating an island in case of contingencies or malfunctions.

1.2.3 Dynamic Security Assessments

Once island candidates have been identified, the feasibility of their secure operation is determined using methodologies and criteria recommended by ENTSO-E. ENTSO-E has made studies recommending appropriate approaches for dynamic security assessments (DSA) that deal with voltage, frequency and angle stability, as seen in Figure 1-2 [6].

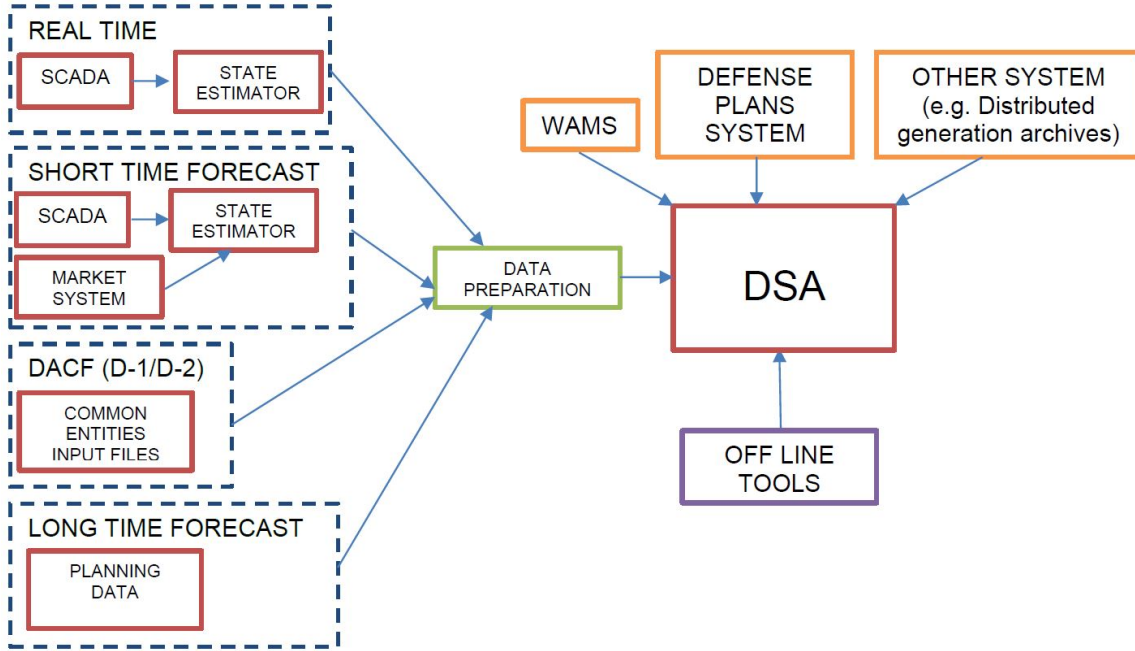


Figure 1-2: Typical workflow for DSA [6]

Generally speaking, power system security is the ability of the system to withstand a specific list of events without the risk of operation disruption [7]. Power system operation works under two types of constraints: load constraints and operating constraints. Load constraints are the load demands that must be met to achieve equilibrium in the system. Operating constraints are maximum and minimum limits of system variables. If both types of constraints are satisfied, system is said to be in a normal operating state. When a disturbance occurs, the system may enter an emergency state if operating constraints are not met, or it may enter a restorative state if load constraints are not met.

A security assessment is a study that checks the ability of a system to withstand events. The system is secure if it can under such disturbance without entering an emergency state. If that's not the case, the system is insecure. ENTSO-E recommends an array of tools for performing security assessments, which range from static, quasi-static to full dynamic studies of the system. For VSAs, PV and QV curves are static tools widely accepted in the industry as graphic representations for indicating if a system is operating in a stable condition and to obtain active and reactive power

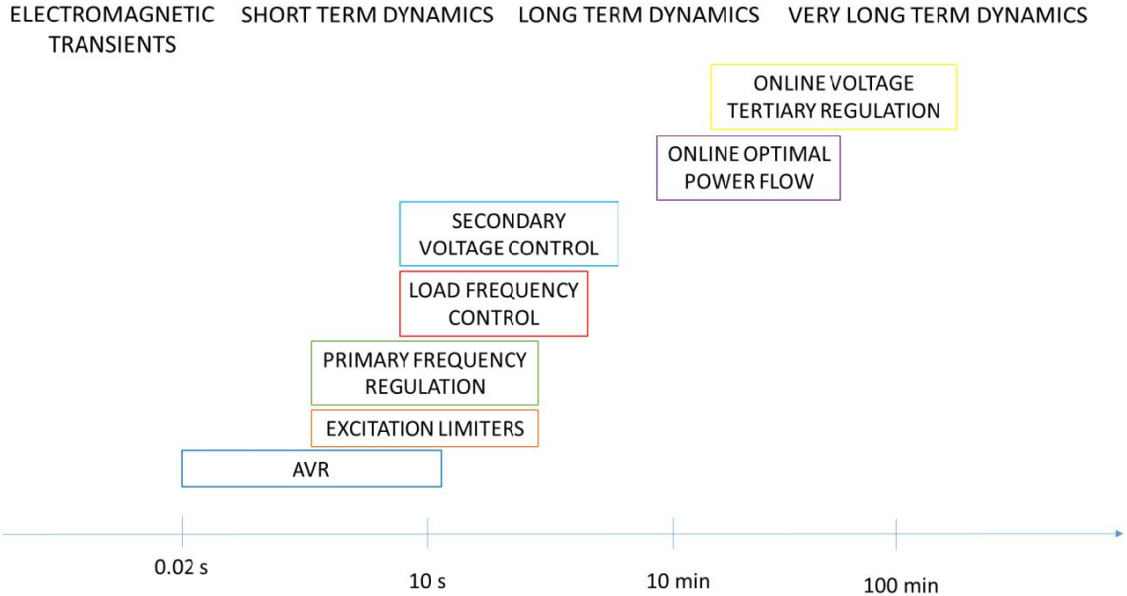


Figure 1-3: Dynamic phenomena in different timeframes [6]

security margins for such system.

FSA tools can use dynamic models and tools to determine the stable and secure operation of a system. These models can gain complexity according to the detail of system topology and according to the timespan studied, as seen in Figure 1-3. Several commercial software packages offer different solutions for dynamic FSA. Depending on the phenomena studied, clients need to determine the scope of their needs and the necessary tools to make appropriate assessments. For FSA purposes, ENTSO-E determines that a single busbar model is sufficient to study dynamic behavior of frequency for different operational scenarios [6, 8, 9]. A single busbar model encompasses a main group of generation connected to a single busbar, feeding a main group of loads. Depending on the timespan to be simulated, different system phenomena and control reactions can be included in the final system model. System phenomena can be inertial response and load-self regulation, while control reactions can be load shedding, primary control, synthetic inertia, amongst others.

Chapter 2

Island Identification

2.1 Description of Algarve Distribution Network

The distribution network (DN) feeding the load centers in Algarve is studied for the scope of this work. The operational information on topology, generation and load of December 2015 is used throughout this project. The Algarve DN is connected to the transmission network (TN) through three main substations, providing electricity at a HV voltage of 60 kV to the distribution network: Estói, Portimão and Tunes [10], as seen in Figure 2-1. These TN substations provide electricity to several DN substations which transform voltage to 15 kV before distributing to the rest of the DN [1].

In [11] several RES are listed in the region, of different technologies: wind, solar, biomass and small hydro. Nevertheless, in the generation information provided for this work, only wind generation is listed as operational and providing active power for the specified dates of study. There are several windfarms in the region, all of them located to the west.

Data on the power consumption and generation was provided by the DSO. The date and time with the maximum load is chosen from the given information, being 01/12/2015 19:15, in order to study a stressed situation of the system. It should be noted that this date is in winter time, and load profile can change in other seasons of the year. The maximum load for the chosen date is of 306 MW and the corre-

Table 2.2: Distribution network substations and associated transmission network substations

Bus ID	Location	Power Demand [MW]	REN Substation
FARO	Faro	13,85	Estói
CMARIM	Castro Marim	1.85	
ALMANCIL	Almancil	8.44	
QUARTEIRA	Quarteira	13.02	
TAVIRA	Tavira	15.31	
TNATAL	Torre Natal	12.15	
OLHAO	Olhão	19.37	
SBALPORTEL	São Brás de Alportel	6.2	
BRACIAIS	Braciais	13.87	
LOULE	Loulé	16.51	
ALDNOVA	Aldeia Nova	14.62	
ARMPERA	Armação de Pera	12.4	Tunes
TUNES	Tunes	9.65	
SBMESSINES	São Bartolomeu Messines	5.91	
ALBUFEIRA	Albufeira	17.49	
MONTECHORO	Montechoro	11.12	
VILAMOURA	Vilamoura	13.71	
CIMPOR	Lameiras	8.92	
SILVES	Silves	6.17	
LAGOA	Lagoa	13.07	Portimão
PLAGOS	Porto de Lagos	12.33	
MONCHIQUE	Monchique	3.17	
STEOTONIO	São Teotonio	6.83	
PORTIMAO	Portimão	21.18	
ALJEZUR	Aljezur	3.04	
LAGOS	Lagos	21.58	
VBISPO	Vila do Bispo	3.77	

2.2 Islanding Detection Techniques

Islanding detection techniques can be categorized in three main types: active techniques, passive techniques and communication-based techniques [12]. Each of these techniques has advantages and disadvantages which were researched. Based on this information a technique was chosen for the scope of this work and proposed for implementation in the Portuguese distribution network.

Passive techniques measure system parameters and compare them to previously determined threshold values to decide if an island is occurring or not. System parameters can be voltage, frequency, rate-of-change-of-frequency (ROCOF), amongst others. One passive technique is over/under-voltage (OVP/UVP) and over/under-frequency (OFP/UFP) measurement. This technique is based on measuring frequency and voltage and determining if values are above or below maximum and minimum thresholds. Although simple in its nature, there are non-detection zones (NDZ) that can be too large for appropriate island detection [13]. Appropriate mathematical models of the existing load and generation would be needed to derive mathematical formula that describes the NDZ. Another technique is based on ROCOF measurement. ROCOF provides a measurement of active power imbalance in a system. If system is stable, small power imbalances will create small transients in the frequency. If there is a sudden important change in active power balance, for example in the case of an islanding event, ROCOF measurements would be high. Should the measurement be higher than a previously established threshold, a relay sends a signal confirming the event and possibly activating associated circuit breakers. Main problem of ROCOF relays though, is that they have been found to be susceptible to false operation, which hinders system reliability [14].

Another type of relays are vector surge (VS) relays, which measure the terminal voltage angle difference in a cycle duration. If there is a sudden change in terminal voltage, its value jumps to another value and the phase changes as seen in Figure 2-2, which is an indicator of an islanding even occurring [14]. The same problem of false operation or unwanted trips noted in ROCOF relays is seen with VS relays.

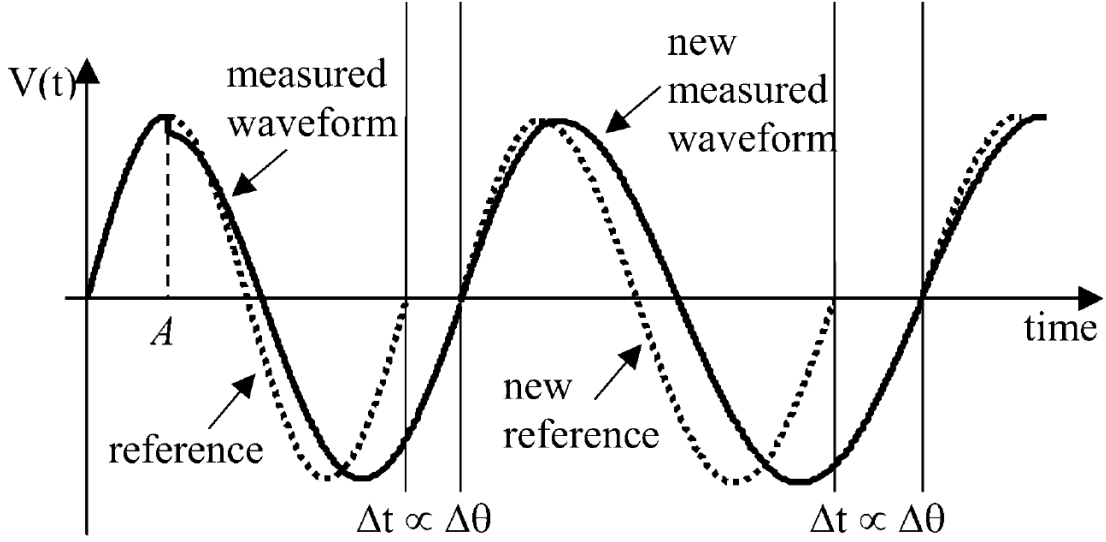


Figure 2-2: Voltage VS [14]

Active techniques involve the intentional injection of small disturbances into the system. Feedback is measured from which an islanding event can be detected. When system is stable, the feedback is negligible. When there is a sudden island, the perturbation will be large enough to create changes in system parameters. Even though these techniques do not have NDZ, the disturbance introduced in the system may incur in power quality problems [12].

Communication based techniques may involve massive installation of PMUs communicated to the SCADA system of the distribution network dispatch center, or it can also involve installation of enhanced communication equipment for existing circuit breakers and DES wherever it is deemed necessary [15]. PMUs provide a very accurate measurement of phasor, frequency and ROCOF synchronized in a time frame usually obtained from GPS signals [5]. These units offer the advantage of very precise measurement, minimize the risk of unwanted trips and their NDZ can be greatly reduced with proper algorithms. Nevertheless, they are currently quite expensive to install in a distribution network in large enough numbers to provide wide coverage.

For the scope and purpose of this work, we consider an offline topological assessment of an existing distribution network. This topological assessment can determine key points in a network where communication devices can be upgraded in order to

assist the dispatch center operator in identifying islanding events. A study based on network configuration does not depend on system parameters and does not suffer from NDZ or power quality issues. Although an installation plan of communication devices in the distribution network would be necessary, an initial wide coverage would not be needed. Only points where feasible live islands may occur would have the proper communication equipment to automatically detect islanding events.

2.3 Proposed Topological Algorithm

Breadth-first search (BFS) algorithm starts with an arbitrary node and explores all the neighboring nodes first before moving to the next level of nodes, as seen in Figure 2-3. Nodes not found in an iteration of this algorithm are considered to be existing in a separate graph. An alternative algorithm is depth-first search (DFS) which starting at an arbitrary node it explores as deep as possible in each branch before returning to the original node level and exploring a new branch in its complete depth.

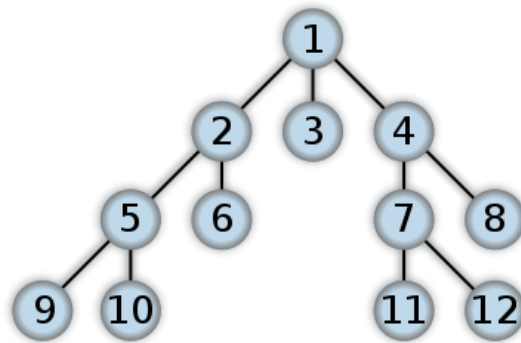


Figure 2-3: BFS order of node traversing [16]

BFS is chosen over DFS because it guarantees completeness, that is, it will eventually find a goal state, where DFS may not find it. BFS also guarantees finding the shortest path between two nodes [17]. This is useful when trying to match the branches of the proprietary DSO file to actual existing lines in the DN.

2.4 Python Script

The database of the DN network in Algarve is provided by the DSO in a proprietary file format. Using this database, we obtain the information on the topology of the system, which consists of 4,541 nodes and 4,426 branches. This database does not have information on load and generation, which is provided in separate Excel databases and is then converted to CSV file format. A Python script is developed that parses through data, creates a graph database and performs a BFS algorithm. General workflow of this script is seen in Figure 2-4. Islands found through this algorithm are checked for power imbalance, given by equation 2.1.

$$P_{imb} = \frac{P_{load} - P_{gen}}{P_{load}} \times 100 \quad (2.1)$$

Maximum power imbalance recommended by ENTSO-E is 40% [8], which is the criteria we will use for considering an island as candidate for feasibility. After identifying island candidates, another Python script creates PSS/E raw files and PYPOWER case format files which are later used for calculating steady state power flow calculations in either commercial or open-source software. PYPOWER is an open-source Python port of the popular MATPOWER MATLAB package.

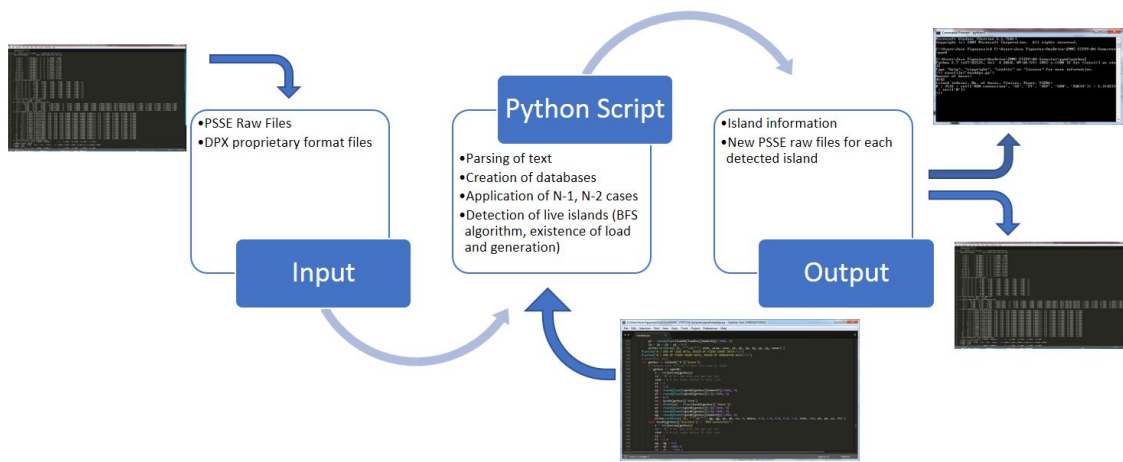


Figure 2-4: Python script workflow

2.5 Results

2.5.1 Topology Analysis Results before N-1 and N-2 Contingency Cases

Before applying N-1 and N-2 contingency cases, the Python script is used to explore distribution network topology as it was provided. The current topology of the network in Algarve is found to be three distinct networks, each independent from each other and connected to a TN substation, which connects them to the transmission network. Even though there are existing physical lines between these different networks, they are normally open. Therefore, in the DN in Algarve we can talk about three main operational islands each associated to the following REN 115/60 kV substations: REN Estói, REN Portimão and REN Tunes.

As mentioned before, all the distributed generation in Algarve is connected to the REN Portimão operational island in the west of Algarve. This means that when applying N-1 and N-2 contingency cases, all the live islands candidates will be found in this specific network.

2.5.2 Topology Analysis Results for N-1 and N-2 Contingency Cases

After applying N-1 contingency cases, no feasible islands were found that also met the criteria of maximum power imbalance of 40%. One possible case is considering the whole electrical island of REN Portimão if the transmission network were to suffer a blackout. This case would create an island with seven main load centers with a total load of 72 MW and seven distributed generation centers with a total generation of 22 MW. This yields a power imbalance of approximately 70%, much higher than criteria used in this study.

When applying N-2 contingency cases only one feasibly island appears as candidate. This island has the Porto de Lagos substation as load center with demand of 12.33 MW and four windfarms as generators: Espinhaço de Cão, Corte dos Álamos,

Bordeira and Guerreiros with 10.55 MW of generation. Power imbalance is therefore of 14.46%. It exists if there were an outage in part of the 60 kV busbar in Porto de Lagos, assuming circuit breakers act fast enough to separate the busbar, along with an outage of line LM60-154 Portimão-Porto Lagos 2. Although this island has a power mismatch below the maximum recommended, a security assessment is performed to determine its secure operation.

For the sake of comparison an additional island has been considered, which exists with N-3 contingency cases. This island has the Vila do Bispo substation as load center with demand of 3.77 MW and two windfarms as generators: Vila do Bispo 2 and Raposeira with 2.51 MW. Power imbalance is therefore of 33.42%. The contingencies needed for this island to exist would be an outage of line LA60-134 Portimão-Lagos, an outage of line LI60-58 Porto Lagos-Lagos I and losing the load of Lagos substation, either by a fault in the associated 15 kV busbar or an outage of the 60/15 kV transformer. This is good example of an island with high power mismatch for which security assessments are needed to determine its secure operation.

Islands' information is summarized in Table 2.3, their geographic location seen in Figure 2-5 and their grid location seen in Figure 2-6.

Table 2.3: Network islands studied in Algarve

Loads	Porto de Lagos	Vila do Bispo
Outages	Part of 60 kV Porto de Lagos busbar	Line LA60-134 Portimão-Lagos
	Line LM60-154 Portimão-Porto Lagos 2	Lagos substation
		Line LI60-58 Porto Lagos-Lagos I
Generating Units	Espinhaço de Cão, Bordeira Corte dos Álamos, Guerreiros	Vila do Bispo 2, Raposeira
Generation Power [MW]	10.55	2.51
Load Demand [MW]	12.33	3.77
Power imbalance [%]	14.46	33.42

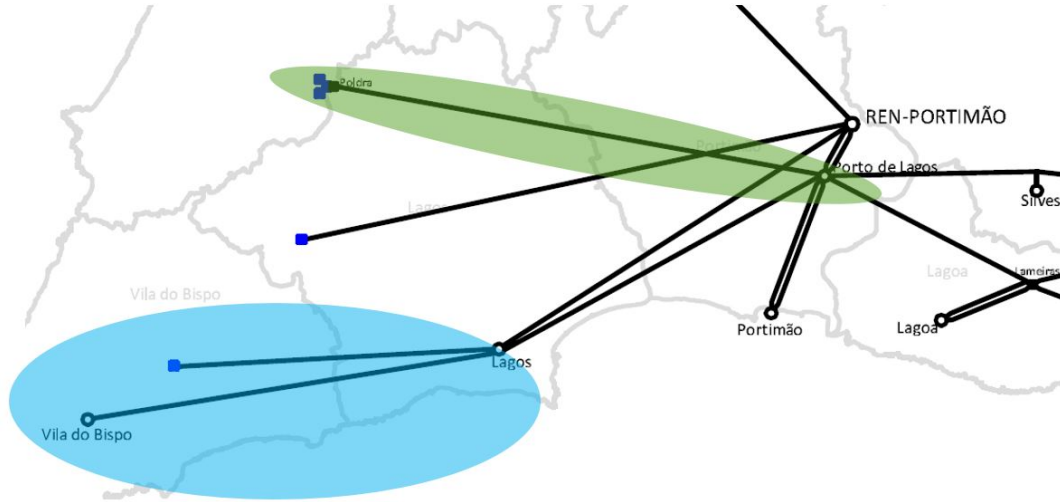


Figure 2-5: Geographic location of islands studied in this work. Green is for the Porto de Lagos island, blue is for the Vila do Bispo island

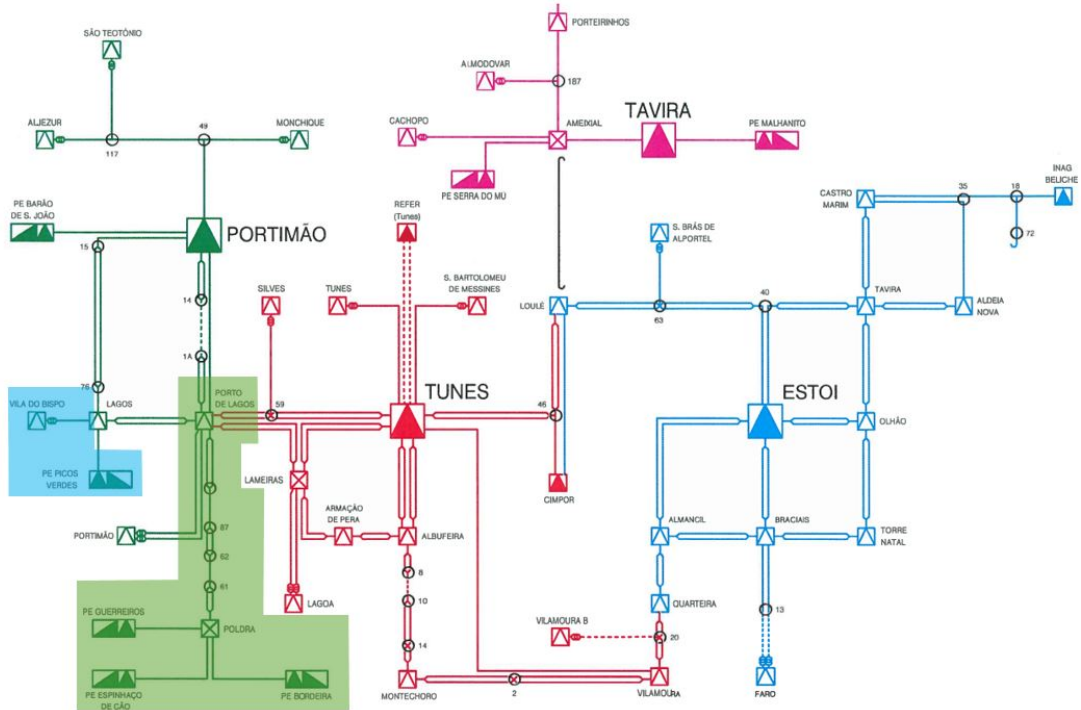


Figure 2-6: Network location of islands studied in this work. Green is for the Porto de Lagos island, blue is for the Vila do Bispo island

Chapter 3

Voltage Security Assessment

3.1 Definition

Voltage security assessment is the evaluation of secure and stable operation of a power system while maintaining acceptable voltage ranges in all the buses of the system after being subjected to a disturbance. This secure state of the system must be maintained in a steady state to be considered stable. Voltage instability occurs when a given load demands more power than what can be delivered by the transmission system and the generators [7]. This event may occur when the power system suffers a disturbance and the voltage value at any of the buses declines in an uncontrollable way. If any of the bus voltages of a power system suffers such decline and values are below secure operational limits, the system may present a voltage collapse. For this work, we define collapse as a catastrophic event that is caused by instability.

The phenomena involved in the voltage stability problem are nonlinear, and as the system experiences more stress, the nonlinearities become more important. There are two types of voltage stability: large disturbance and small disturbance. Large disturbance voltage stability involves major events such as system-wide faults, sudden loss of generators or loads, etc. Small disturbance voltage stability involves small changes in the system due to load dynamics or control actions.

To determine the feasibility of an island in a grid, voltage stability must be studied. This can be done either in a static or dynamic model. Static tools depend on steady

state power flow calculations. Dynamic analysis includes generator dynamics, tap changing transformers and detailed control system models. Steady state calculations involve solution of algebraic equations, which simplifies computational workload and is less thorough than dynamic analysis. It is difficult to analyze all the factors associated to this nonlinear phenomenon using one model or set of techniques, especially when working with distribution network where all the information may or may not be readily available to dispatch center operators. Being that detailed models are not available for all the DES in a distribution network, and the computational resources available for such networks could be limited, in this work we propose the use of static tools to analyze long term voltage stability. Long term stability ultimately determines if a given island can operate in a secure voltage range.

There are two types of graphs widely accepted in the industry for analyzing long term stability mechanisms: PV and QV curves. In both techniques, load flow equations are solved for long-term equilibrium for different values of active and reactive power injection to load. When using numerical algorithms to solve these equations and there is no convergence to a solution, it most probably means that an equilibrium does not exist. This divergence is found graphically in the PV and QV curves. These curves are considered cases of continuation methods.

Continuation methods compute solutions for equations corresponding to a range of values of a certain parameters. These methods start from a base case to a loadability limit. This method is also called continuation power flow. Numerically, a predictor-corrector scheme is used which involves a logic that changes the continuation parameter if a convergence problem arises. The loadability limit is detected when the continuation parameters starts decreasing, indicating that the lower solution of the graph is being calculated now. After this point is reached, there is little interest to continue the calculation because the loadability limit, which is of main interest, has been found. PV and QV curves are described in more detailed in the next sections, showing them as cases of continuation methods.

3.2 Mathematical Derivation of PV and QV Curves

Let us consider a single-load, infinite-bus system, such as the one in Figure 3-1. In this system, we assume a balanced 3-phase system, therefore a single line diagram will be sufficient as representation. The infinite bus is represented by a generator which has a voltage magnitude of E and is chosen as the slack bus, therefore its angle will be 0. The transmission line is represented by a resistance R and a reactance X . The generator is providing power to a load with an active power P and a reactive power Q , which is connected to a bus with a voltage magnitude of V and a phase angle of θ .

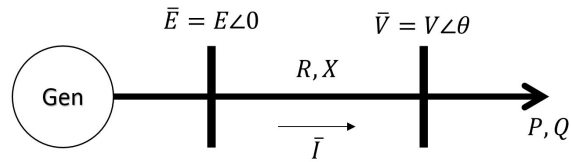


Figure 3-1: Single line representation of single-load, infinite-bus system

Being that the resistance of transmission lines is often neglectable when compared to the reactance, we can obtain equation 3.1 from Figure 3-1:

$$\bar{V} = \bar{E} - jX\bar{I} \quad (3.1)$$

The complex power consumption of the load can be expressed using equation 3.2:

$$S = P + jQ = \bar{V}\bar{I}^* = \bar{V} \frac{\bar{E}^* - \bar{V}^*}{-jX} = (EV \cos\theta + jEV \sin\theta - V^2) \frac{j}{X} \quad (3.2)$$

Expression 3.2 can be further decomposed into real and imaginary parts to obtain expressions for active and reactive power:

$$P = -\frac{EV}{X} \sin\theta \quad (3.3)$$

$$Q = -\frac{V^2}{X} + \frac{EV}{X} \cos\theta \quad (3.4)$$

Equations 3.3 and 3.4 are the power flow equations of a lossless system. Given values of P and Q they can be solved with respect to V and θ . Eliminating θ from equations 3.3 and 3.4 yields the following:

$$(V^2)^2 + (2QX - E^2) V^2 + (P^2 + Q^2) X^2 = 0 \quad (3.5)$$

Equation 3.5 is a second-order equation with respect to V^2 , which needs the following condition to have at least one solution:

$$(2QX - E^2)^2 - 4X^2 (P^2 + Q^2) \geq 0 \quad (3.6)$$

Assuming condition 3.6 holds, the two solutions of expression 3.5 are given by:

$$V = \sqrt{\frac{E^2}{2} - QX \pm \sqrt{\frac{E^4}{4} - X^2 P^2 - X E^2 Q}} \quad (3.7)$$

From equation 3.7 we can derive that for a given load power, there are two solutions, one with higher voltage and lower current, and another with lower voltage and higher current. The solution with higher voltage and lower current is considered to be a normal operating condition, where load bus voltage V , is closer to generator voltage E . Operation in the lower solutions range is not considered to be a stable operation, as will be discussed in the following sections.

Considering equation 3.7, with a constant Q , V can be plotted with respect to P creating PV plots, as later shown in Figure 3-2. Otherwise, considering a constant P , V can be plotted with respect to Q creating QV plots, as later shown in Figure 3-3.

3.3 PV Curves

PV curves can give a good understanding of long-term instability [7]. These curves are a graphical representation of the relationship between active power and voltage in a given bus. These can determine voltage stability either in a radial or meshed network. It is performed in a power flow simulation by increasing power at a given system by steps, establishing beforehand generator buses and load buses. Voltage is measured at a previously established critical bus and is then plotted against the power injected in to the system.

The solution is nonlinear, and for each value of active power below the maximum there are two solutions, one with high voltage and the other with low voltage. The solution of higher voltage corresponds to normal operation. This region of the curve shows a stable behavior, where an increase in load demand will create a decrease in voltage. As power draws near to maximum value, it is said to be in the “knee” of the curve, where voltage drops very rapidly when power increases. This drop in voltage would rapidly increase the current injection in the bus and stress the system to a state of near-collapse. With increased currents, active power losses in cables increase, introducing more thermal stress to the cables and increasing the voltage drop even more.

At the maximum limit, power flow solution fails to converge, which indicates instability. The other region of the curve, with the low voltage solution, presents an unstable behavior. In this region, an increase in power creates an increase of voltage, and a decrease of power creates a decrease of voltage. If the base operation point is found to be in this region, the system is unstable and voltage collapse is imminent. Active power security margin, or loadability limit can be considered as the difference between active power injection in operating condition and maximum active power.

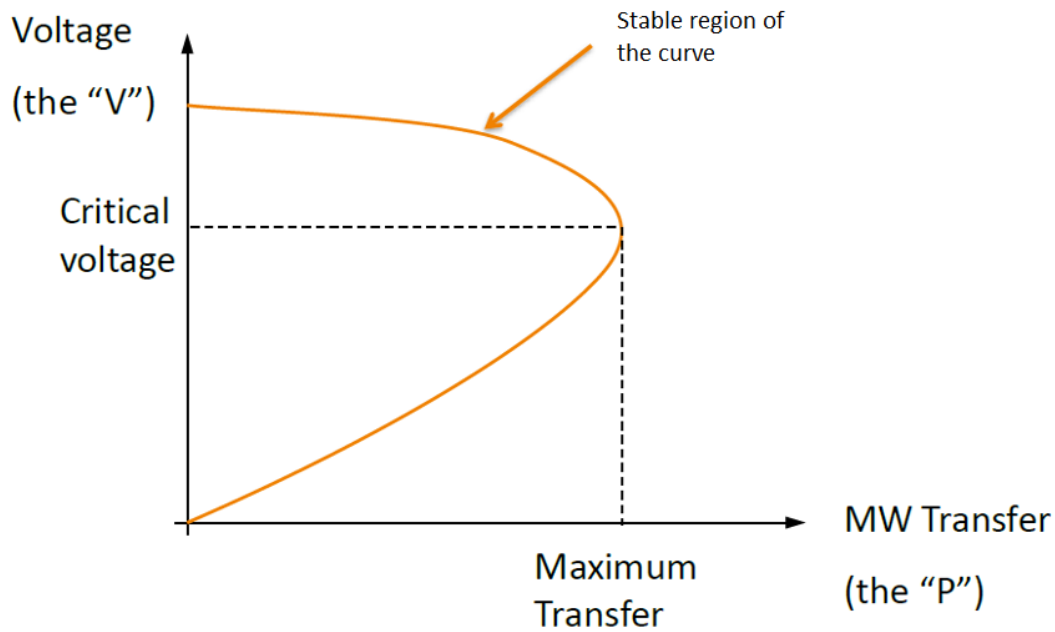


Figure 3-2: PV curve [18]

3.4 QV Curves

QV curves are the relationship between reactive power injection and voltage in a bus. Even though it is called a QV curve, a normal convention is that the vertical axis holds the values of reactive power and the horizontal axis is the voltage for the reactive power condition. It is determined by connecting a fictitious generator to the analyzed bus. This generator has zero active power and produces any value of reactive power to meet a voltage set-point. The voltage set point is varied and the reactive power production is recorded. The base case will be when the fictitious generator is at 0 MVAR output, which is the original state of the system. A decrease in the generator output corresponds to an increase of the reactive power of the load.

Similarly to the PV curve, there is a maximum value reached at this case, at the “bottom” of the curve, where if reactive power is to increase any more, a voltage collapse would occur. When voltage levels are about to reach the “bottom” of the curve, voltage drops rapidly with a change in reactive power injection, which

would rapidly increase the current injection in the bus and stress the system to a state of near-collapse. With increased currents, active power losses in cables increase, introducing more thermal stress to the cables and increasing the voltage drop even more.

If the QV curve does not cross the horizontal axis, it is an unsolvable case and the system analyzed has collapsed. Additional reactive power injection is needed for the system to operate. When a system is found with a base case in the left side of the curve, an increase of reactive power load would actually increase the voltage, resulting in an unstable behavior, and voltage collapse would be imminent. Reactive power security margin or loadability limit can be considered as the distance between maximum reactive power value found at the “bottom” of the curve and the horizontal axis which indicates the operating condition.

Besides security margins for reactive power, QV curves can also provide values for shunt compensation for the system to reach a specified voltage. These curves would vary depending on the position of the shunt, which would require a previous decision on which bus it would be connected to.

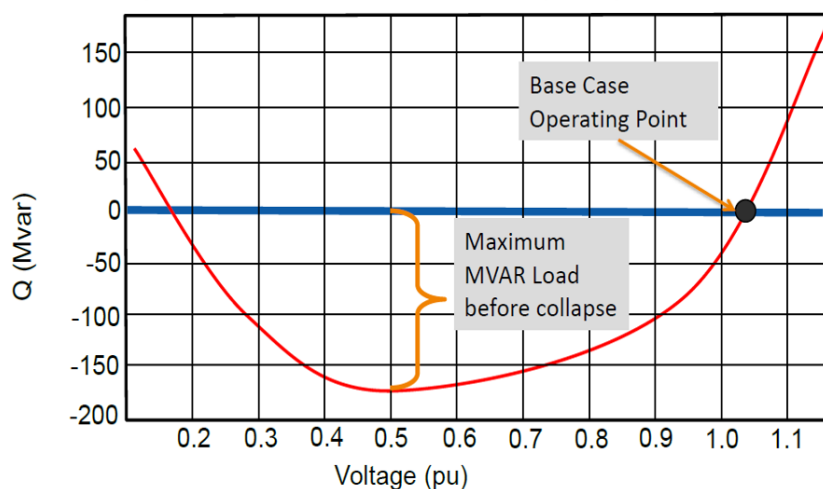


Figure 3-3: QV curve [19]

3.5 Results of PV and QV Curves

PV and QV curves were plotted for the two previously established island candidates, the Porto de Lagos island and the Vila do Bispo island. As it is to be expected in simple systems such as these ones, power flow solutions performed on both of the previous the islanding events, and after the islanding events assuming that generators provide necessary power, show that the buses with lowest voltage value will be the load buses. Therefore, PV and QV curves are created for these buses. Even though PSS/E raw files are used and created by automated Python scripts beforehand, PowerWorld is chosen to plot PV and QV curves due to its user-friendly interface for creating these graphs.

For PV plots, injection buses are chosen to be the generator buses, and sink buses are chosen to be the load buses as these present the lowest voltage values both before and after islanding event. These graphs are calculated until the maximum capacity of the generators is reached, or until it fails to converge, indicating voltage collapse. QV plots are plotted for any range of voltage values until its maximum allowed value of 1.1 pu. This is done in the load buses due to same reasons explained for PV plots. In the following subsection results are shown for each island and security margins are summarized in Table 3.1.

3.5.1 Porto de Lagos Island PV and QV Results

For the Porto de Lagos island, the operation point is found to be in a stable region for both PV and QV curves. Active power security margin is limited only by the maximum power capacity of the wind farm generators, and is approximately 40 MW, as seen in Figure 3-4. Reactive power security margin is approximately 65 MVAR, as seen in Figure 3-5.

3.5.2 Vila do Bispo Island PV and QV Results

For the Vila do Bispo island, the operation point is also found to be in a stable region for both PV and QV curves. Active power security margin is limited only by the

maximum power capacity of the wind farm generators, and is approximately 11 MW, as seen in Figure 3-6. Reactive power security margin is approximately 35 MVAR, as seen in Figure 3-7.

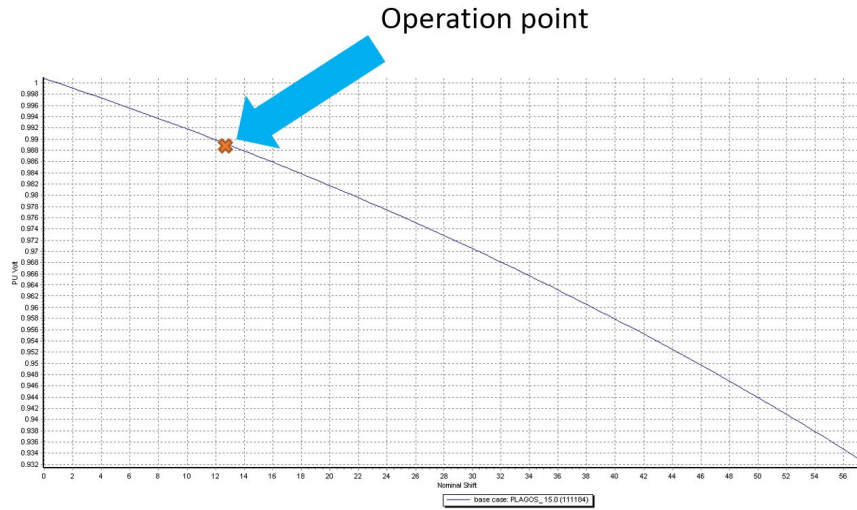


Figure 3-4: Porto de Lagos island PV curve

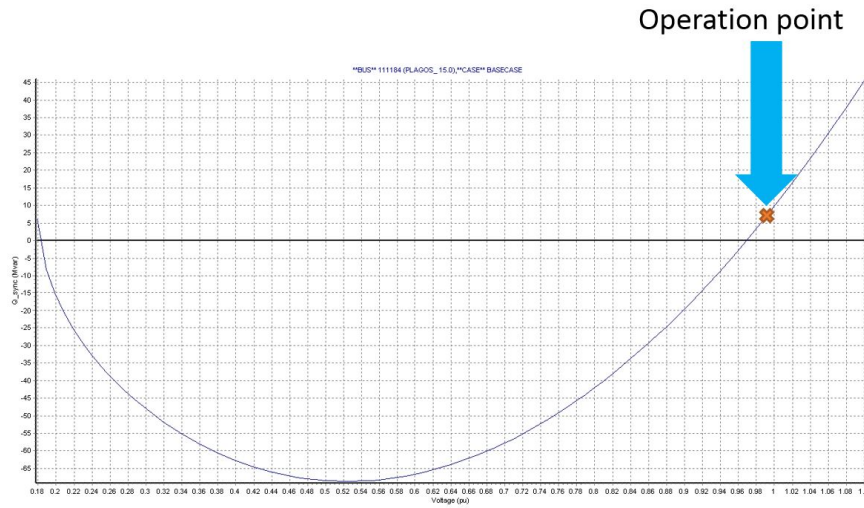


Figure 3-5: Porto de Lagos island QV curve

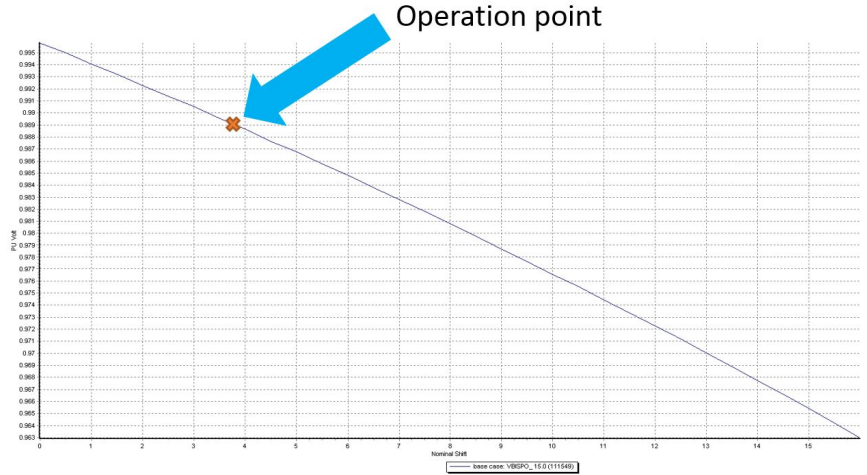


Figure 3-6: Vila do Bispo island PV curve

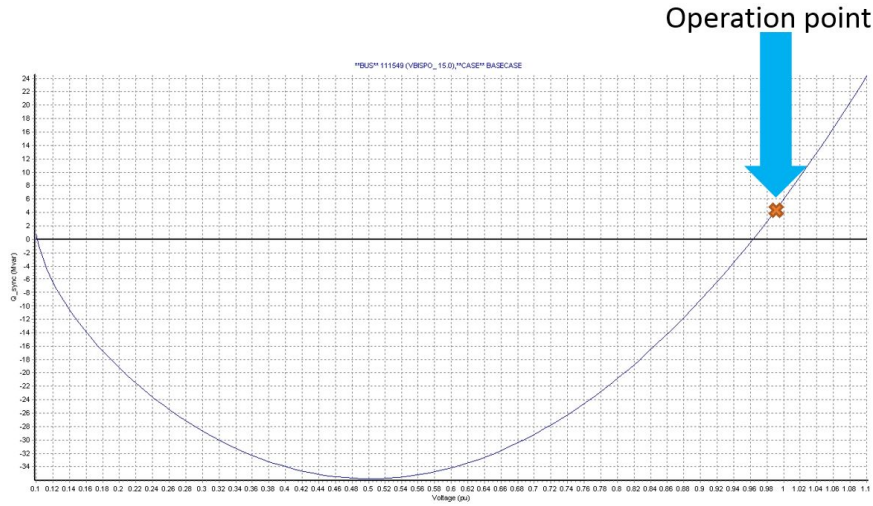


Figure 3-7: Vila do Bispo island QV curve

Table 3.1: Active and reactive power security margins of studied systems

Electrical island	Active Power Security Margin [MW]	Reactive Power Security Margin [MVAR]
Porto de Lagos	40	65
Vila do Bispo	11	35

Chapter 4

Frequency Security Assessment

Grid frequency is normally directly related to the rotating speed of synchronous generators. Being that these synchronous generators are rotating masses, there is an associated kinetic energy stored within them. This kinetic energy is a function of the moment of inertia of the rotors and the rotating speed. When the system does not have any power mismatch between load and generation, there is no acceleration or deceleration in the rotational speed. Any deviations on the frequency is a response to power mismatches in the system. When there is more generation power than load demand, this translates to an acceleration in the rotational speed and therefore in the system frequency. In the opposite scenario, there is less generation power than load demand, which translates to a deceleration in the frequency.

The most frequent phenomenon is the sudden loss of generation, which can create a dangerous decay of frequency and ultimately collapse the system. Synchronous generators have different response mechanisms to these frequency deviations. In the first instances after the contingency, the inherent inertia of the rotors releases the kinetic energy stored in their masses [20]. This kinetic energy prevents the frequency from immediately collapsing after a power mismatch provoked by loss of generation. Depending on the amount of kinetic energy on the system, this inertial response can allow for the other response mechanisms to actuate in due time. After approximately 1 to 10 seconds, primary control, in the form of governor actuation, reacts to inject more active power to the system and try to arrive to zero power mismatch. This

would lead to a stabilized frequency that is not the nominal one. After a few seconds, secondary control or automatic generation control kicks in. This control corrects the steady state error that the frequency may have and leads it to a nominal value.

In current power systems, there is a decrease of inertia as generation is shifting from a classical synchronous generation to a non-synchronous generation. This decrease of inertia must be addressed to maintain system security. Inertial response is not natural or must be implemented in other ways in wind generators. Being that all wind generators are either asynchronous or completely decoupled from grid frequency, they do not react automatically to frequency excursions outside a nominal value. Different control strategies have been investigated and implemented in the industry, allowing for wind generators to provide inertial response, primary control and secondary control to support grid frequency and power mismatches.

According to ENTSO-E, the main parameter to be considered for frequency stability criteria is the admissible rate of change of frequency (ROCOF). According to their simulations, the future grid should be able to handle a ROCOF of 2 Hz/s and a power imbalance of 40% [8]. The higher the ROCOF, the less stable the power system will be. High ROCOF mean that large transients of voltage angles could occur in different zones of the grid and induce pole slipping on synchronous generators and network splitting.

A frequency security assessment (FSA) is made for the network islands found in this work. This assessment involves a dynamic model of the system that includes the phenomena that are for interest for the scope of this project. For an island to be feasible, FSA should determine that a minimum frequency of 47.5 Hz is not reached after islanding event, and that maximum ROCOF does not exceed ENTSO-E recommendations, as higher values could lead to instabilities of the system.

4.1 Model Description

In this work, a single busbar model is chosen for dynamic simulations, which is stated as valid in several ENTSO-E studies [6, 8, 9]. In this model, a single generation mass

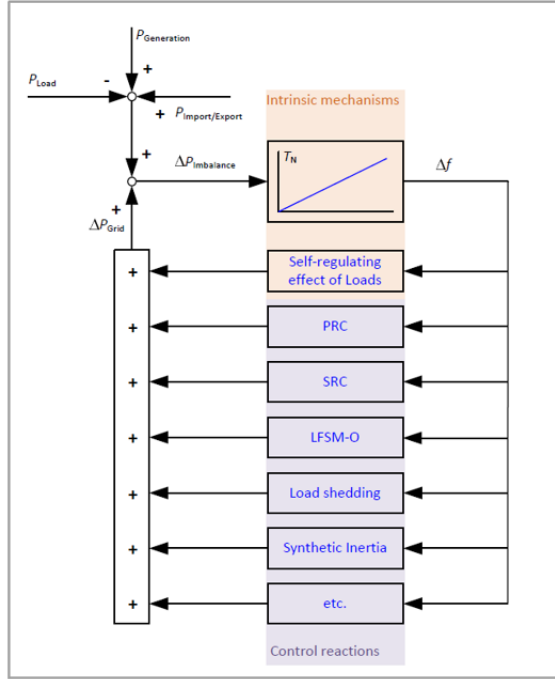


Figure 4-1: Block diagram of single busbar model [8]

is connected to a single load mass by means of a single busbar, and power balance depends solely on generation and demand. There are several dynamic phenomena that can be included in this model, described by ENTSO-E in Figure 4-1.

Dynamic phenomena in the single busbar model can be either intrinsic mechanisms or control reactions. The intrinsic mechanisms of this model are system inertia, which provides kinetic energy from rotating masses, and self-regulating effect of loads, which describes the effect of energy interchange between the load and the system to stabilize the frequency. Control reactions include primary reserve control (PRC), secondary reserve control (SRC), limited frequency system mode for over-frequency (LFSM-O), under-frequency load shedding (UFLS), synthetic inertia, etc.

Depending on the timeframe of simulation, some of these mechanisms or reactions have certain influence on system behavior. If the simulation is to last for several minutes, these effects must be considered. In Figure 4-2 timeframes are shown where these effects have more influence or start to act.

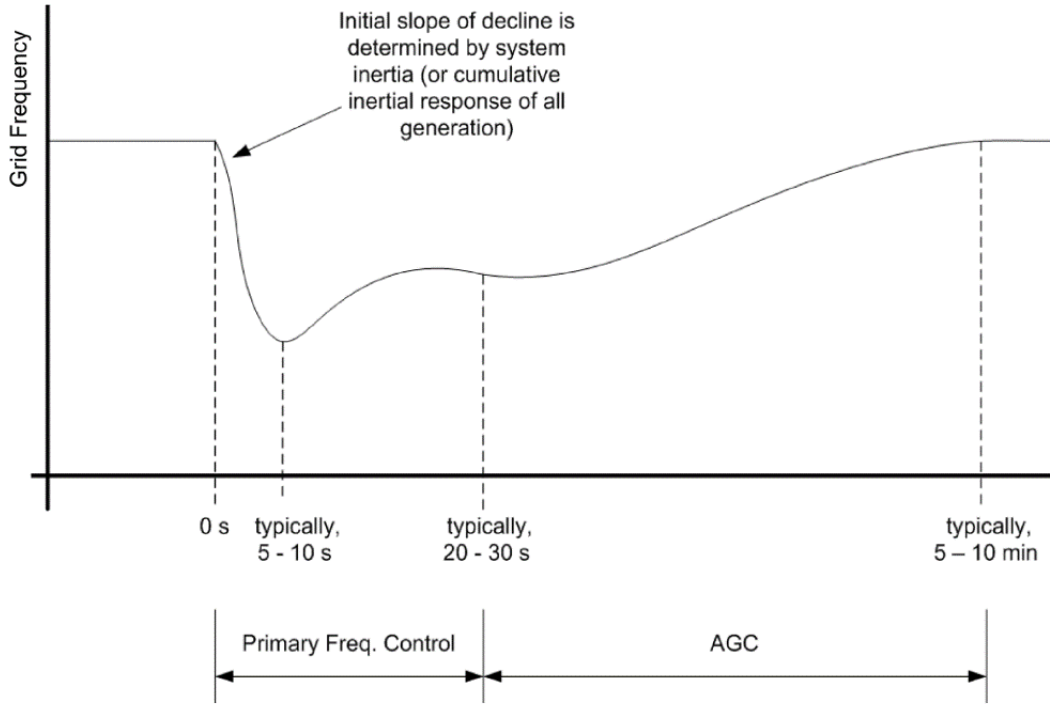


Figure 4-2: Response time of frequency-related mechanisms and reactions [20]

4.2 Inertial Response

Immediately after a change in frequency, the rotors of synchronous generators release or absorb kinetic energy. This inertial response is intrinsic in conventional synchronous generators. The swing equation describes this mechanism, which shows that a net accelerating torque is produced when there is a difference between mechanical torque of generator shaft and electrical torque:

$$T_a = T_m - T_e \quad (4.1)$$

T_m is mechanical torque, T_e is electrical torque and T_a is accelerating torque [N·m].

The differential equation that considers rotor dynamics, total moment of inertia I [kg·m²] of the synchronous machine and angular displacement θ_m [rad] with respect to the stationary reference axis in the stator is:

$$I \frac{d^2 \theta_m}{dt^2} = T_m - T_e \quad (4.2)$$

Knowing that rotor angular velocity ω_m is:

$$\omega_m = \frac{d\theta_m}{dt} \quad (4.3)$$

We can reformulate equation 4.2 as:

$$I \frac{d\omega_m}{dt} = T_m - T_e \quad (4.4)$$

Multiplying expression 4.4 by ω_m we obtain:

$$I\omega_m \frac{d\omega_m}{dt} = \omega_m T_m - \omega_m T_e \quad (4.5)$$

Torque multiplied times angular velocity is power, therefore the swing equation can be written as:

$$I\omega_m \frac{d\omega_m}{dt} = P_m - P_e = P_k \quad (4.6)$$

Where P_k [W] is the power that comes from kinetic energy given by inertial response. Integrating both sides of equation 4.6 over a specific window of time yields:

$$W_k = \frac{1}{2} I \omega_m^2 \quad (4.7)$$

Equation 4.7 is the final expression of kinetic energy given by system inertia, where W_k [J] is the kinetic energy of rotational masses. Kinetic energy can also be expressed in terms of an acceleration time constant and nominal power:

$$W_k = GH \quad (4.8)$$

Where G is nominal power [W] and H is inertia constant or acceleration time constant [s]. It is worth noting that different authors use different variables for these measurements, and may include different constant values like $H/2$ instead of H .

4.3 Load Self-Regulation

During an event of frequency deviation, the load exchanges energy with the system. This can be considered a regulating effect of the load that finally stabilizes the system frequency. Basically, the load changes its power consumption in direct proportion to a change of frequency. When this change is considered, the power needed from kinetic energy is reduced as the load reduces its power demand.

From equation 4.6 we can consider the following expression of power imbalance:

$$\Delta P = P_m - P_e \quad (4.9)$$

Considering the decrease of power consumption due to load self-regulation, and the fact that the change of energy over time is power, which was already considered for equation 4.7, we can have the following expression:

$$P_k = -\frac{dW_k}{dt} = \Delta P - K_r \Delta f \quad (4.10)$$

Where K_r is the self-regulation coefficient and Δf [Hz] is the change in frequency. The self-regulation coefficient can be calculated as:

$$K_r = \frac{P_e}{f} \quad (4.11)$$

4.4 Under Frequency Load Shedding

According to ENTSO-E [9], under frequency load shedding (UFLS) is a control strategy that represents middle term between quasi-linear control and a rigid fixed load disconnection. A well designed UFLS scheme should have the capacity to compensate for active power deficit in an appropriate window of time to allow system recovery by slower control reactions such as PRC and SRC. Only a minimum shedding of load should be needed to allow for this compensation. When correctly implemented it must either avoid network islanding or allow for control of network islanding events.

One important parameter to consider is frequency range of UFLS scheme. The

first step of shedding step is usually 49 Hz. This allows for a range of 1 Hz between 50 Hz and 49 Hz that can be used by PRC to recover the system, or by the system operator to compensate for power imbalances. The last shedding step is usually 48 Hz, which allows for 1 Hz range to control frequency transients by shedding load. Below the 48 Hz threshold there is a 0.5 Hz margin that allows generating units to recover without finally tripping at 47.5 Hz. Relay delay time should be considered. Relays always have an intrinsic delay as they take time to perform internal computations and then open the circuit breaker. Intentional delay above the 49 Hz threshold can be added too if it exists or is being designed for. Frequency drops even lower than intended threshold due to this delay.

Another important parameter is the number of shedding steps, which is directly related to the total load to be shed. ENTSO-E recommends a maximum of 50% of reference load and a minimum of 40% of minimum load to be shed. The number of shedding steps would depend on the percentage shed per each step to reach the total percentage. For the two network islands identified and described in Chapter 2, there is an existing UFLS scheme which sheds approximately 10% of the load in two frequency thresholds, as shown in Table 4.1.

Table 4.1: Existing UFLS scheme in Portimão substation, which serves loads in Porto de Lagos and Vila do Bispo

Frequency [Hz]	Load shed [%]
48.6	10
48.4	10

In this work, another UFLS scheme is considered, to serve as comparison against the existing one. UFLS plans with non-linear load shedding steps have been shown to not being able to reach a system balance. Therefore, a symmetrical UFLS scheme is proposed, considering that in each step the amount of load to be shed should be between 5% and 10%. In Table 4.2 a plan of action is proposed, which follows all previously mentioned recommendations. Although minimum number of steps should be 6, number of steps are here studied is 5, as a compromise between ENTSO-E recommendation and current scheme in operation shown in Table 4.1. In this way,

a total load shed of 50% can be achieved in symmetrical steps of 10%. This plan is chosen due to precedents of previous events in which existing UFLS plans consisting of shedding of less than 10% per step were not able to recover the system fast enough for PRC to act and finally stabilize the system [21].

Table 4.2: Proposed UFLS scheme

Frequency [Hz]	Load shed [%]
48.8	10
48.6	10
48.4	10
48.2	10
48.0	10

4.5 Synthetic Inertia

Inertial response is not natural or must be implemented in other ways in wind generators. Being that all wind generators are either asynchronous or completely decoupled from grid frequency, they do not react automatically to frequency excursions outside a nominal value. Different control strategies have been investigated and implemented in the industry, allowing for wind generators to provide inertial response, primary control and secondary control to support grid frequency and power mismatches.

According to the IEEE PES Wind Plant Collector System Design Working Group, there are five types of WTGs [22]. These are categorized according to the generator technology and their connection to the grid. Type 1 generators, described in Figure 4-3, are asynchronous machines that are directly connected to a step-up transformer and afterwards to the grid. The turbine speed is close to grid frequency. Active power is generated when turbine shaft rotates faster than grid frequency, creating a negative slip. Type 2 generators, described in Figure 4-4, are asynchronous machines directly connected to the grid with a variable resistor and possibly power electronics connected to the rotor circuit. This allows for rotor current control and limited speed control by creating higher slips.

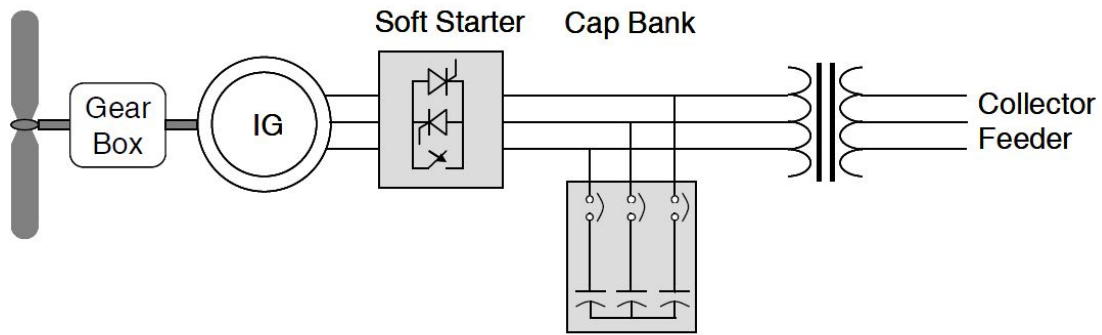


Figure 4-3: Typical WTG Type 1 configuration [22]

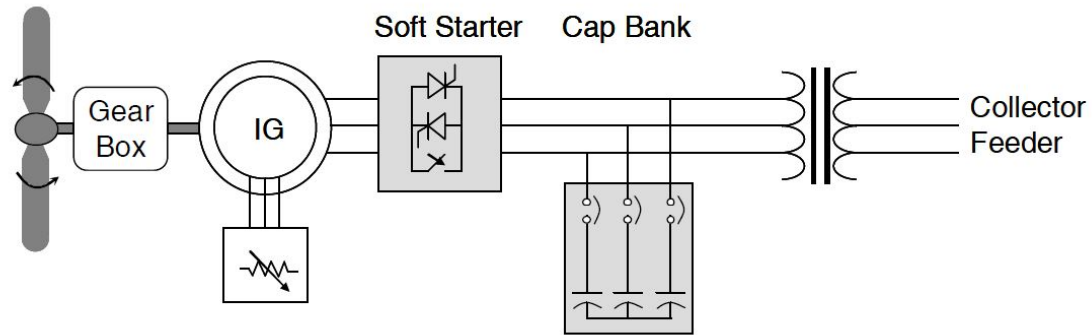


Figure 4-4: Typical WTG Type 2 configuration [22]

Type 3, described in Figure 4-5, generators are doubly-fed induction generators, with a stator directly connected to the grid and the rotor connected to the grid through a back to back power converter. This power converter adds variable AC excitation to the rotor circuit, and are rated for up to 30% of the rating of the generator. Power flows in or out the rotor circuit and allows for a wider speed range, approximately up to 50% higher and lower of synchronous speed.

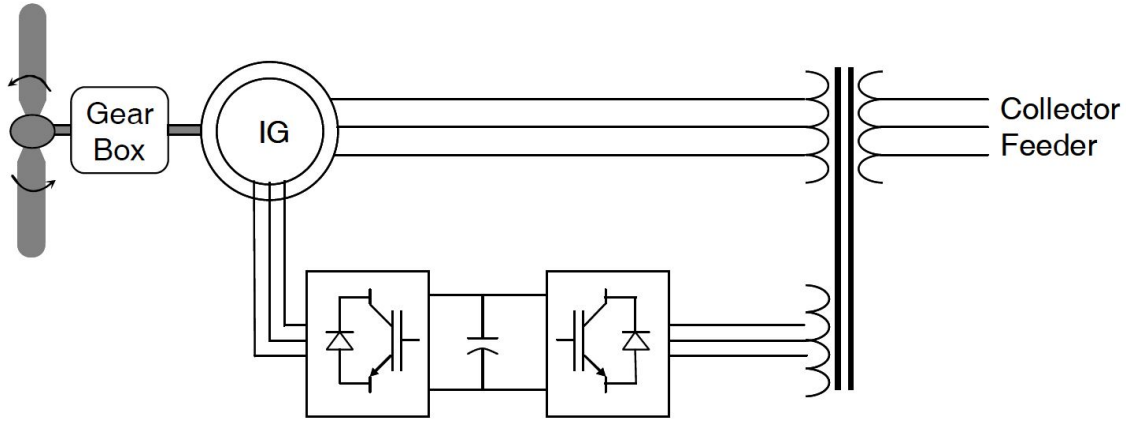


Figure 4-5: Typical WTG Type 3 configuration [22]

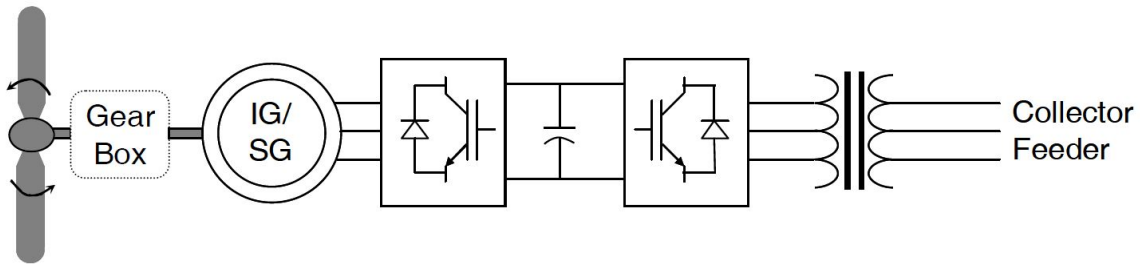


Figure 4-6: Typical WTG Type 4 configuration [22]

Type 4 generators, described in Figure 4-6 can be either synchronous or asynchronous machines which are allowed to rotate at any aerodynamically efficient speed. Generally no gearboxes are used, with either wound rotor synchronous machines or permanent magnet synchronous machines directly coupled to the turbine shaft. The stator is connected to the grid by means of a 100% rated back to back power converter, which converts the changing AC frequency of the generator to the fixed AC frequency of the grid.

Finally, Type 5 generators, described in Figure 4-7, are synchronous generators directly connected to the grid, and coupled to a torque/speed converter which converts the changing turbine shaft speed to a constant output shaft speed.

None of the discussed types of WTGs offer a direct coupling between turbine rotational speed and grid frequency. Types 1 and 2 depend on a difference of speed known as slip to inject (or absorb) power from the grid. They do provide some frequency

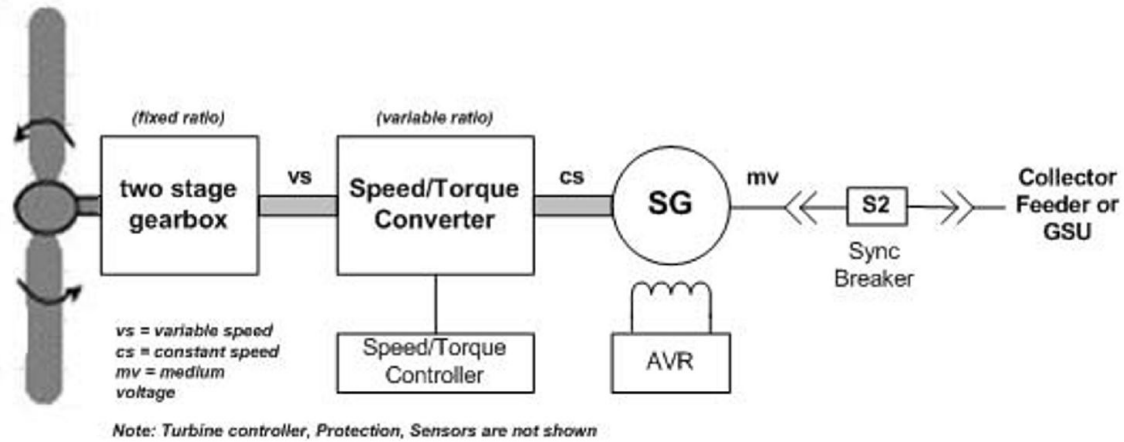


Figure 4-7: Typical WTG Type 5 configuration [22]

support [23], but it is not automatic and takes some time to release the kinetic energy, depending on the power mismatch between generator and turbine. Types 3 and 4 let the turbine have a totally different speed, which tends to be aerodynamically efficient. Finally Type 5 uses a torque/speed converter to convert turbine shaft's rotational speed to synchronous frequency.

Table 2.1 shows that all DES in Algarve are WTGs of Type 3 or Type 4. Therefore, if frequency suddenly changes due to power mismatch, the kinetic energy of the rotational inertia will not be automatically extracted to support frequency, even though it still exists stored in the rotational inertia. The extraction of this kinetic energy is offered by several manufacturers using different control strategies in their power converters [24, 25]. These control strategies are called synthetic inertia, as they emulate the inertial response of a synchronous generator even if the generator is non-synchronous.

Synthetic inertia response is part of a wider active power control that manufacturers can provide. Nevertheless, if the service is not provided or contractually enforced, WTGs will not support the grid during frequency deviations. Manufacturers commonly offer the service of providing approximately 10% of rated power for a time-span of 5 to 10 seconds, and some also offer either a surge of additional 10% of active power, or a load-following active power control that can last for a time-span of 5 to 10 seconds.

4.6 Excel/VBA Tool

A tool was made in Microsoft Excel which uses calculations done in spreadsheets, whose outputs are inputs for a Visual Basic for Applications (VBA) code. Excel was chosen because it is widely available and it is a power mathematical tool, especially when combined with VBA, which allows for iterative code. This is ideal for dynamic simulations which require many calculations for a specific number of time steps.

The first sheet of the tool is the “Parameters” sheet, shown in Figure 4-8. This sheet shows the color code for user input cells that will be used throughout the tool’s sheets. Orange is used for necessary user input, and blue is used for optional user input that allows for improved accuracy of results. Any other colors are not user input cells. A cell of special interest is the adjustment for the self-regulation coefficient, whose default value is 1.0, which allows for empirical adjustment of such coefficient if needed.

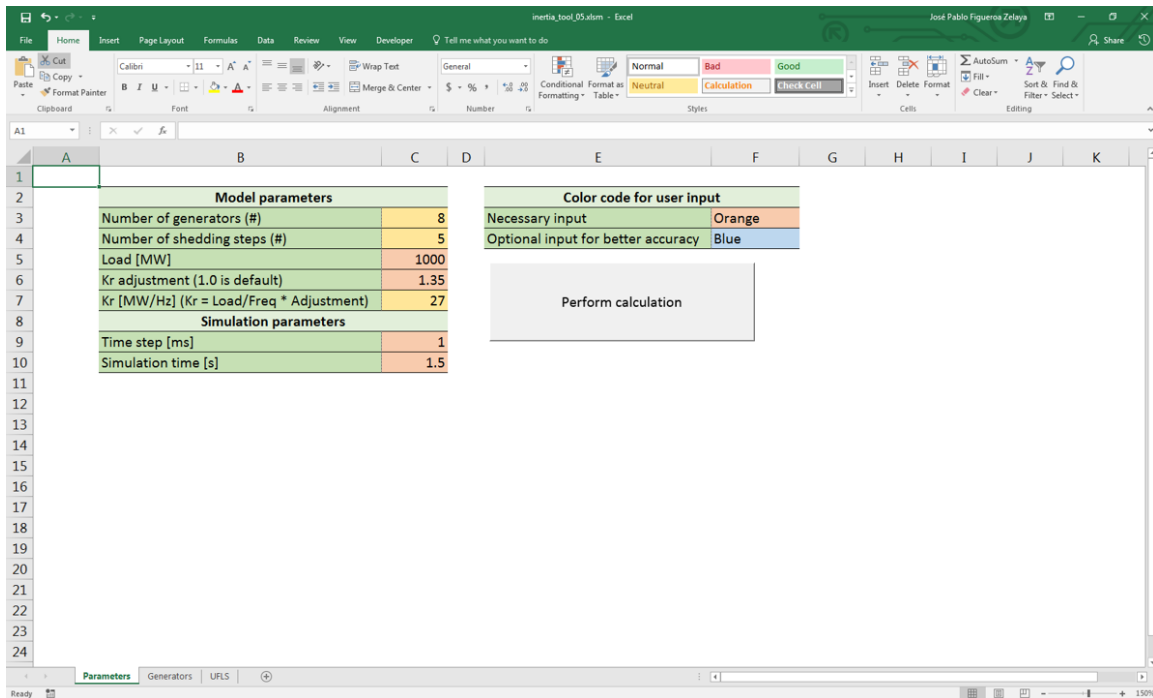


Figure 4-8: Parameters sheet of Excel tool

The second sheet of the tool is the “Generators” sheet, shown in Figure 4-9. This sheet allows the user to input information of existing generators in the system.

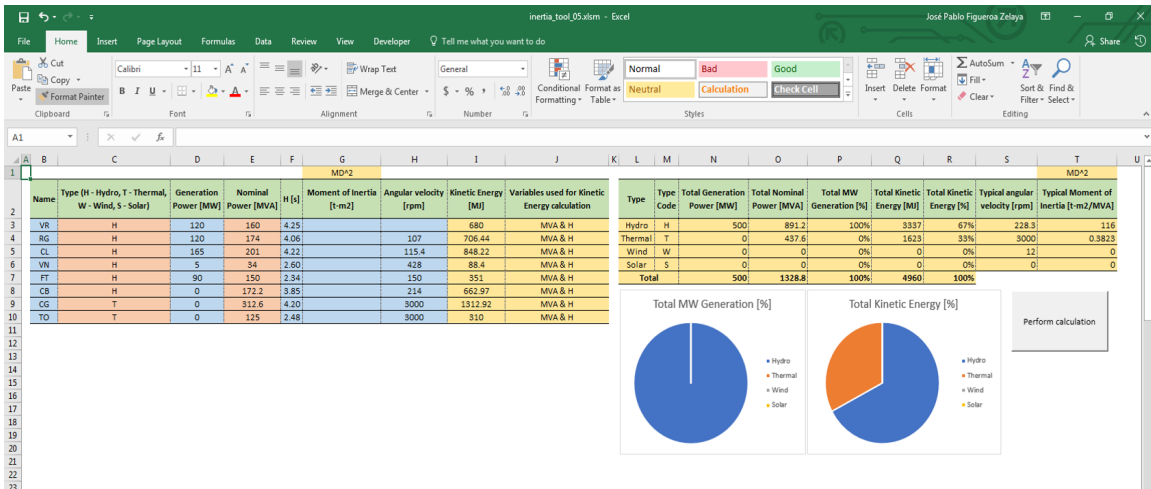


Figure 4-9: Generators sheet of Excel tool

Necessary information includes the type of generation and the nominal power of the generating unit. From this information, kinetic energy can be calculated by using typical values for different types of generation already stored in the tool and shown in this sheet. Optional user input is generation power, acceleration time constant, moment of inertia and angular velocity. When given this optional information, the tool can calculate kinetic energy per generator in an accurate way. The VBA tool will later calculate for any missing values in optional user input cells.

This sheet shows graphic information of generator participation in active power generation and kinetic energy contribution, as well as tabular information of generation according to its type. Some generation can contribute to kinetic energy but not to active power generation if the generators are working as synchronous reactive power compensators. Therefore, the graphs of total active power generation and total kinetic energy contribution may differ.

The third and final input sheet of the tool is called the UFLS sheet, shown in Figure 4-10. This sheet contains the information of how much active power demand and generation is shed for specified frequency steps. Relay delay is also specified to add better accuracy to the model. In this delay value, both intentional and intrinsic delays can be considered.

Under-frequency load shedding				
	Frequency [Hz]	Load Shed [MW]	Gen Shed [MW]	Relay Timer [s]
Initial condition	50	0	0	0
	49	190	0	0.15
	48.8	140	0	0.5
	48.7	25	0	0.5
	48.5	85	0	0.5
	48.4	60	0	0.5

Figure 4-10: UFLS sheet of Excel tool

To implement the previously described model for FSA, a mathematical expression was derived which considers the system inertia and load self-regulation. Being that rotor angular velocity is directly proportional to network frequency:

$$\omega_m = 2\pi f/p \quad (4.12)$$

Where p is number of pairs of poles in a synchronous generator. Therefore, equation 4.7 can be rewritten as kinetic energy being directly proportional to system frequency squared:

$$W_k = a f^2 \quad (4.13)$$

Constant a can be calculated from equation 4.13:

$$a = W_k/f^2 \quad (4.14)$$

Equation 4.10 can be rewritten using expression 4.13 as:

$$P_k = -\frac{dW_k}{dt} = \Delta P - K_r \Delta f = -2af \frac{df}{dt} \quad (4.15)$$

Knowing that $\Delta f = 50 - f$:

$$df/dt = -d\Delta f/dt \quad (4.16)$$

Another term can be created to further simplify equation 4.15:

$$T = 2af \quad (4.17)$$

This term T can be considered constant in order to maintain the frequency above the 47.5 Hz threshold. To do this, \bar{f} is used instead of f , where $\bar{f} = 0.98 \times 50$ Hz and is defined as the average frequency value.

Equations 4.16 and 4.17 are substituted in equation 4.15 and yield the following:

$$P_k = -\frac{dW_k}{dt} = \Delta P - K_r \Delta f = T \frac{d\Delta f}{dt} \quad (4.18)$$

Which can be expressed as:

$$\frac{d\Delta f}{dt} = \frac{1}{T}(\Delta P - K_r \Delta f) \quad (4.19)$$

The solution for the differential equation 4.19 is the following:

$$\Delta f = \frac{\Delta P}{K_r} [1 - e^{-(K_r/T)t}] \quad (4.20)$$

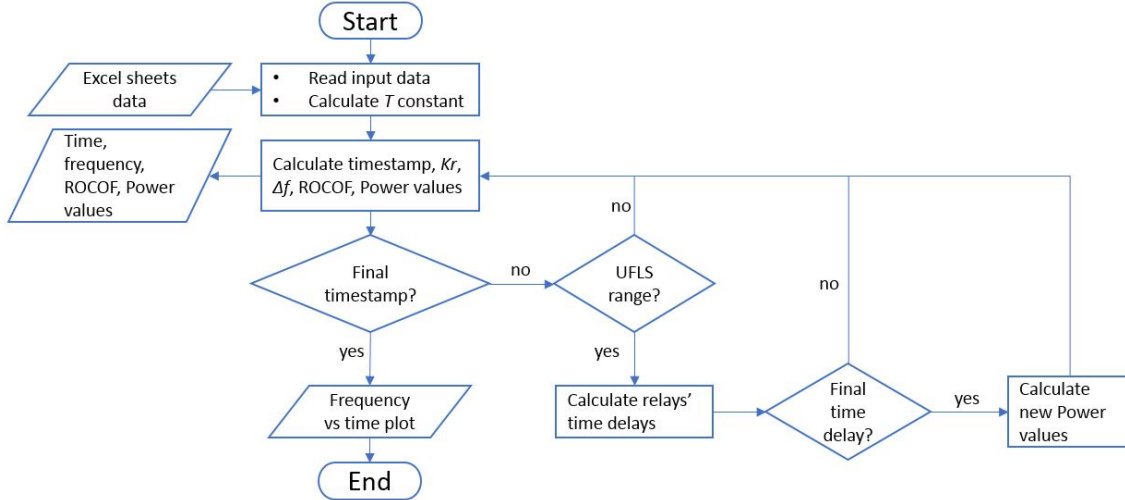


Figure 4-11: VBA code flowchart

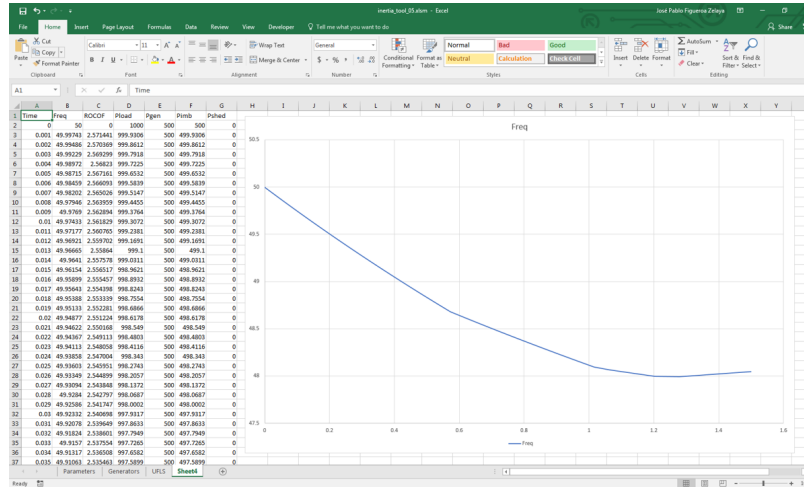


Figure 4-12: Output sheet of Excel tool after VBA code is run

Equation 4.20 is the main expression used in the VBA code of the tool. This VBA code takes the input from the Excel sheets and calculates equation 4.20 for every time step. If a frequency value is reached that matches a threshold of the UFLS scheme, load and/or generation is shed after a certain time delay has passed. The VBA code can be found in the Appendix, and its flowchart is shown in Figure 4-11.

The code is run once a button is pressed, which is found in all the Excel sheets. An example of code output is shown in Figure 4-12, which corresponds to the input shown in Figures 4-8, 4-9 and 4-10.

4.7 FSA Results

To consider a system feasible in an FSA, the following requirements have been specified: existing inertia response and an UFLS plan either to completely avoid reaching 47.5 Hz threshold and set the system on path to recovery, or to allow enough time as shown in Figure 4-2 for other slower control reactions to react and recover the system without reaching the 47.5 threshold. For all UFLS cases, an intrinsic relay delay time has been assumed equal to 2 cycles. Another requirement is that ROCOF would ideally be less than maximum recommended by ENTSO-E of 2 Hz/s. Values higher than this one may incur in unrecoverable unstable system.

The Excel/VBA tool is used for FSA in both islands identified and summarized in Table 2.3. As previously mentioned, all DES in Algarve are WTGs of either Type 3 or Type 4. This means that if those turbines have not been enabled to provide synthetic inertia response, they will not help the system recover in case of islanding events, and they will therefore disconnect automatically from the grid without providing any frequency support. Islanding would not be possible in this scenario. Different other scenarios are modelled for comparison.

For this study, synthetic inertia response has been assumed available in the generating units of the studied islands. Although it is out of the scope of this work to evaluate control strategies to provide this response, it has been mentioned that many manufacturers offer the service of surge of kinetic energy equivalent of 10% of nominal power for 10 seconds. To quantify this kinetic energy, equation 4.8 can be used:

$$W_k = 0.1 \times G \times 10 \quad (4.21)$$

Which can be expressed as:

$$W_k = G \times 1 \quad (4.22)$$

Where acceleration time constant can be taken as 1 s.

4.7.1 Scenario 1

For Scenario 1, information of Table 2.3 as well as assumptions of equation 4.22 are input in “Generators” sheet of Excel/VBA tool. Existing UFLS plan of Table 4.1 is used in UFLS sheet.

Tool outputs the following results for the Porto de Lagos island:

- The isolated group of Porto de Lagos will have a maximum ROCOF of 4.3 Hz/s.
- ROCOF higher than recommended maximum may cause the system to become unstable.
- The current UFLS plan is adequate enough to recover the system and give time for PRC to react, if instabilities due to high ROCOF allow, as shown in Figure 4-13.

Tool outputs the following results for the Vila do Bispo island:

- The isolated group of Vila do Bispo will have a maximum ROCOF of 12 Hz/s.
- Very high ROCOF will most probably cause the system to become unstable.
- The current UFLS plan is not adequate enough to recover the system before any other control reaction acts, as shown in Figure 4-14.

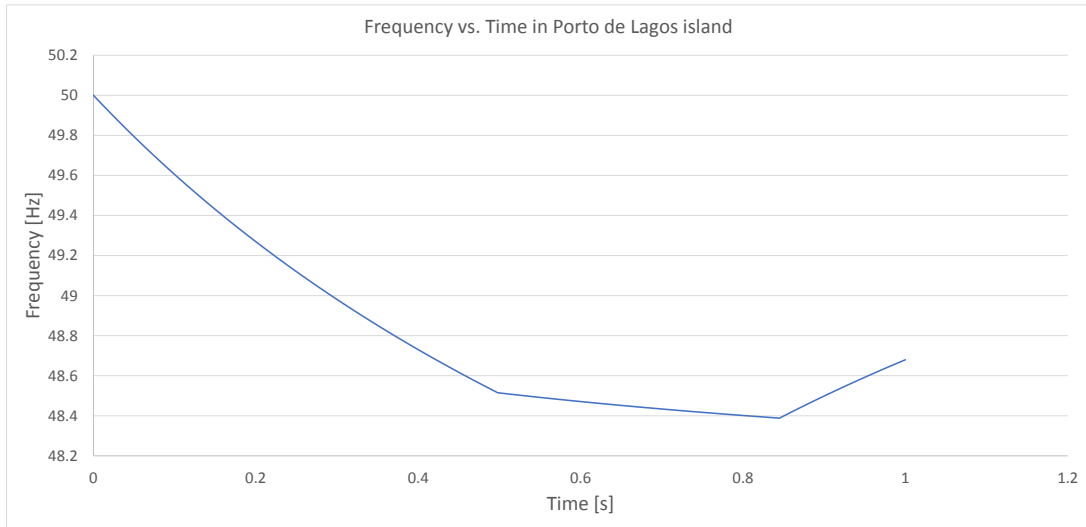


Figure 4-13: Output plot for Porto de Lagos island, Scenario 1

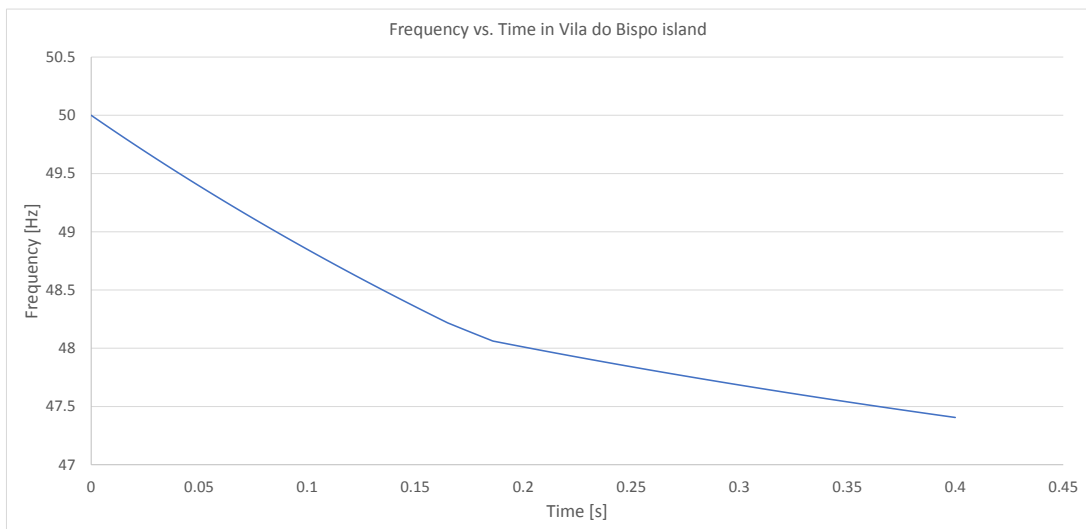


Figure 4-14: Output plot for Vila do Bispo island, Scenario 1

4.7.2 Scenario 2

For Scenario 2, information of Table 2.3 as well as assumptions of equation 4.22 are input in “Generators” sheet of Excel/VBA tool. Nominal power is increased by 10%, as seen in some manufacturers literature, having $G_{new} = 1.1 \times G_{prev}$. Existing UFLS plan of Table 4.1 is used in UFLS sheet.

Tool outputs the following results for the Porto de Lagos island:

- The isolated group of Porto de Lagos will have a maximum ROCOF of 1.6 Hz/s.
- ROCOF below the recommended maximum means the system will be stable.
- The current UFLS plan is adequate enough to recover the system and give time for PRC to react, as shown in Figure 4-15.

Tool outputs the following results for the Vila do Bispo island:

- The isolated group of Vila do Bispo will have a maximum ROCOF of 9.3 Hz/s.
- Very high ROCOF will most probably cause the system to become unstable.
- The current UFLS plan is not adequate enough to recover the system before any other control reaction acts, as shown in Figure 4-16.

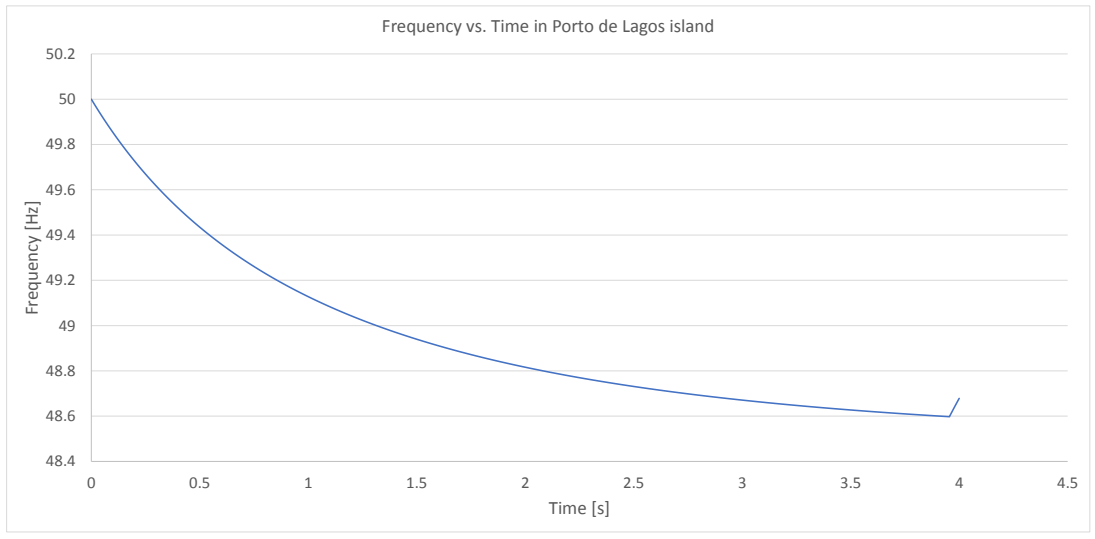


Figure 4-15: Output plot for Porto de Lagos island, Scenario 2

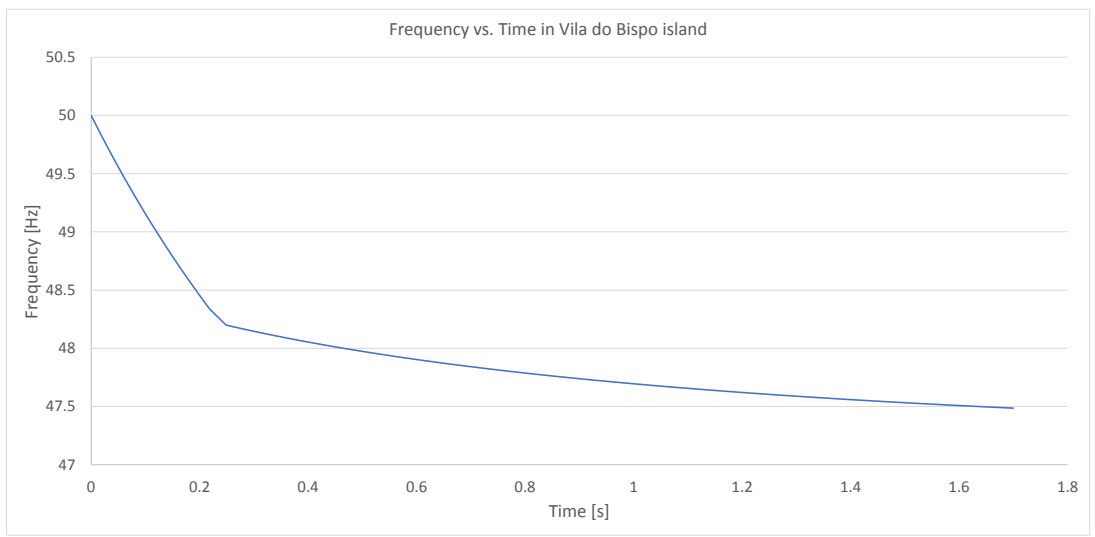


Figure 4-16: Output plot for Vila do Bispo island, Scenario 2

4.7.3 Scenario 3

For Scenario 3, information of Table 2.3 as well as assumptions of equation 4.22 are input in “Generators” sheet of Excel/VBA tool. Nominal power is increased by 10%, as seen in some manufacturers literature, having $G_{new} = 1,1 \times G_{prev}$. Proposed UFLS plan of Table 4.2 is used in UFLS sheet, adding more shedding steps.

Tool outputs the following results for the Porto de Lagos island:

- The isolated group of Porto de Lagos will have a maximum ROCOF of 1.6 Hz/s.
- ROCOF below the recommended maximum means the system will be stable.
- The proposed UFLS plan is adequate enough to recover the system and gives more time for PRC to react, as shown in Figure 4-17.

Tool outputs the following results for the Vila do Bispo island:

- The isolated group of Vila do Bispo will have a maximum ROCOF of 9.3 Hz/s.
- Very high ROCOF will most probably cause the system to become unstable.
- The proposed UFLS plan could recover the system and give time for PRC to react, if instabilities due to high ROCOF allow, as shown in Figure 4-18.

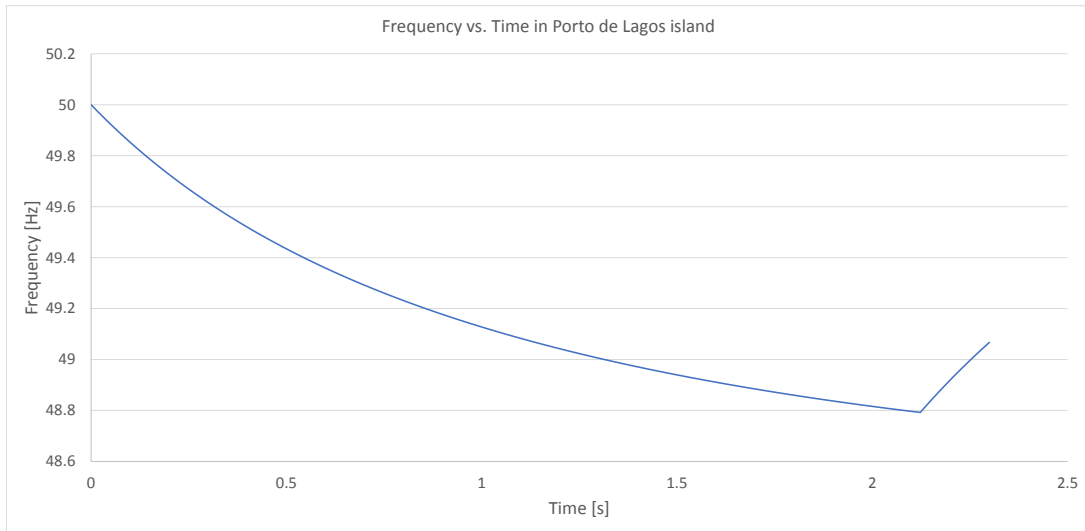


Figure 4-17: Output plot for Porto de Lagos island, Scenario 3

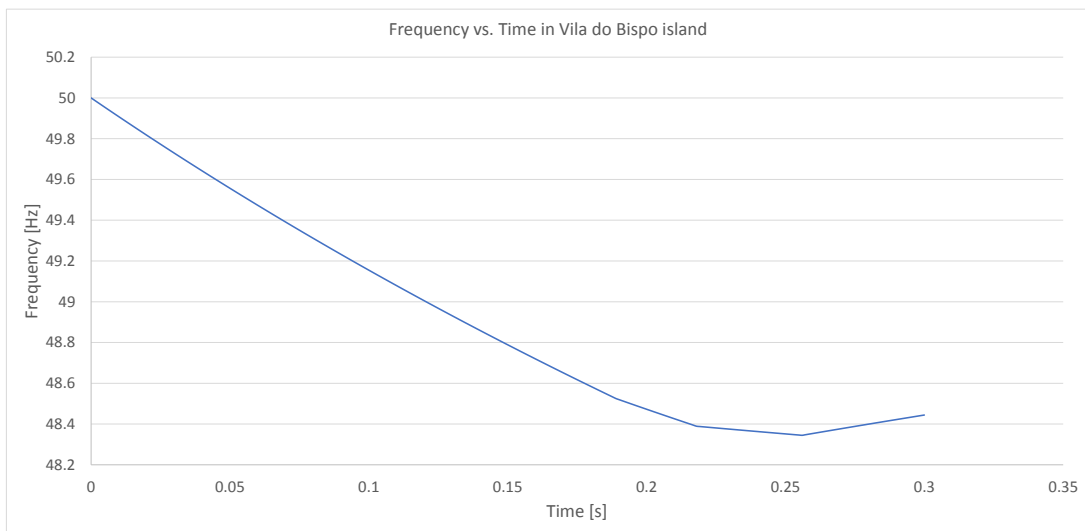


Figure 4-18: Output plot for Vila do Bispo island, Scenario 3

Chapter 5

Conclusions, Recommendations and Future Work

5.1 Conclusions

This thesis presents the work of smart grid security analysis with renewable energy. With every increasing penetration of DES, security analysis should be done at the distribution level following guidelines that already exist at transmission level. This is due to the influence of such distributed generation on the voltage and frequency security of the overall system. If DES coming from RES are to provide support for grid operation, the DSO dispatch center should be ready to act accordingly and have the necessary tools to assess the correct operation of their area of responsibility. One of the challenges that arises with this evolving grid is the security of live islands. Nowadays islanding is altogether eliminated by the DSO due to technical and economic reasons, preventing the generating units to provide support to TSO grid and curtailing customers of electrical energy in case of contingencies. This work proposes a workflow to analyze system security in a grid after islanding events, to contribute to the development of an ever-smarter grid.

In Chapter 2, an offline topological assessment is proposed for the distribution network in Algarve. This assessment uses Python scripts using mainly breadth-first search algorithms to search for island candidates, independently of the amount of

buses and equipment the system may be composed of. This script allows for parsing of PSS/E raw files or the more complex DPX proprietary format. Automatic generation of either PSS/E raw files or PYPOWER case files is introduced in the script, which is used in further automation scripts in PYPOWER library and psspy module for PSS/E to evaluate power flow solutions which can be used for security assessments. Using N-1 and N-2 contingency cases, only one feasible island is found with Porto de Lagos as load. The constraint of power imbalance being less than or equal to 40% drastically reduces the possibility of feasible islanding in the Algarve region. For the sake of comparison, another island is studied which is only possible under an N-3 contingency case, with Vila do Bispo as load. Offline topological studies can determine in which part of the network would enhanced communication devices be a priority and which generation could be subject to islanding events.

In Chapter 3, a voltage security assessment is performed and described. Industry-wide accepted techniques of PV and QV plots were used to assess for voltage security of the islands found in Chapter 2. The theory behind such plots is explained, and after performing steady state power flow solutions on the studied systems using PYPOWER and PSS/E for comparison, load buses are determined to have the lower voltage and the most probable ones to suffer insecure operation due to out of range voltages. PV and QV plots are generated at load buses using PowerWorld software. After obtaining such plots, very wide security margins are found for voltage operation, only limited by the generating units' maximum capacity.

In Chapter 4, a frequency security assessment workflow is proposed. After describing the model used for this assessment, an Excel/VBA tool is described, which was developed for the purpose of this thesis. Excel/VBA was chosen due to its wide availability in the industry, therefore available to operators and analysts alike without having to incur into higher costs for dynamic simulation packages of other software vendors. Phenomena such as inertia, load self-regulation and control reactions such as UFLS are modelled in this tool. Being that WTGs are the only type of generating units found at distribution level in Algarve, synthetic inertia was introduced by quantifying the amount of kinetic energy the manufacturers have demonstrated

in the literature. It was shown that under current UFLS plan in those load centers, only the Porto de Lagos island with 14.46% power imbalance could have the chance of surviving. Chances increase with an additional surge of kinetic energy that some manufacturers can offer. Another UFLS plan is proposed that closely resembles ENTSO-E recommendations and could even make the Vila do Bispo island feasible with its 33.42% power imbalance.

5.2 Recommendations

After obtaining the results summarized in the Conclusions, the following recommendations can be made:

- A plan can be performed to improve protection scheme against unwanted islanding, and enhance system for future operation of such isolated system. This plan must include reliable communication with equipment that is found in offline studies to be critical for islanding prevention and/or operation.
- UFLS can be changed to another one with more shedding steps, such as the one proposed in this thesis in Chapter 4. This could enable more feasible islands with higher power imbalances and improve security of existing feasible ones. Furthermore, by having a more aggressive UFLS plan, generators can be expected to operate in a more secure way during contingency events, providing much needed support to the grid.
- Immediate implementation of 47.5 to 51.5 Hz operating range mandated in the RfG code can be applied to all WTGs that contribute to system inertia, having been proved that their contribution even allows handling of islanding events should they occur.
- Once islands are controlled, automatic reconnection rules can be applied [3], to work towards a smarter grid with higher penetration of renewable energy sources connected at the distribution network level.

5.3 Future Work

The work towards a smarter, safer grid should be ongoing. After having written this thesis, many possible lines of future work come to mind, such as:

- Introduce more detailed generation governor control into the Excel/VBA tool.
- Introduce other control strategies into the Excel/VBA tool, such as secondary reserve control.
- Research of safe automatic reconnection rules for islanding events.
- Study the implementation of dynamic VSA that is computationally efficient for operators to use.
- Assess the use of energy storage for improving overall grid security at distribution level.
- Present the results of this work as scientific papers in journals and/or conferences.

Appendix A

VBA code

```
Function COF2(Pimb As Double, Pload As Double, f As Double, TN As Double, kr As
    Double, t As Double)
    ' This function calculates the change of frequency, taking into account
    ' inertia and load self-regulation

    COF2 = (Pimb / kr) * (1 - Exp(-t * kr / TN))

End Function

Function TN(numgen As Integer, freq0 As Double)
    ' This function calculates T constant based on information given in the
    ' "Generators" Worksheet

    Dim genpn As Double, geninertia As Double, genangvel As Double, genenergy As
        Double, genh As Double, i As Integer, totenergy As Double

    ThisWorkbook.Sheets("Generators").Select
    ThisWorkbook.Sheets("Generators").Range(Cells(3, 6), Cells(numgen + 2, 8)).Font.
        Bold = False

    For i = 1 To (numgen)
        genenergy = ThisWorkbook.Sheets("Generators").Cells(i + 2, 9)
        ' Check which cells are empty and calculate energy accordingly
        If IsEmpty(ThisWorkbook.Sheets("Generators").Cells(i + 2, 6)) Then
            ThisWorkbook.Sheets("Generators").Cells(i + 2, 6) = ThisWorkbook.Sheets("
                Generators").Cells(i + 2, 9) / ThisWorkbook.Sheets("Generators").
                Cells(i + 2, 5)
            ThisWorkbook.Sheets("Generators").Cells(i + 2, 6).Font.Bold = True
        End If
        If IsEmpty(ThisWorkbook.Sheets("Generators").Cells(i + 2, 8)) And Not (
```

```

IsEmpty(ThisWorkbook.Sheets("Generators").Cells(i + 2, 7)) Then
ThisWorkbook.Sheets("Generators").Cells(i + 2, 8) = genenergy * (8000 /
    ThisWorkbook.Sheets("Generators").Cells(i + 2, 7)) / ((2 *
    WorksheetFunction.Pi / 60) ^ 2)
ThisWorkbook.Sheets("Generators").Cells(i + 2, 8).Font.Bold = True
ElseIf IsEmpty(ThisWorkbook.Sheets("Generators").Cells(i + 2, 7)) And Not (
IsEmpty(ThisWorkbook.Sheets("Generators").Cells(i + 2, 8))) Then
ThisWorkbook.Sheets("Generators").Cells(i + 2, 7) = genenergy * 8000 / ((
    ThisWorkbook.Sheets("Generators").Cells(i + 2, 8) * 2 *
    WorksheetFunction.Pi / 60) ^ 2)
ThisWorkbook.Sheets("Generators").Cells(i + 2, 7).Font.Bold = True
ElseIf IsEmpty(ThisWorkbook.Sheets("Generators").Cells(i + 2, 7)) And IsEmpty
(ThisWorkbook.Sheets("Generators").Cells(i + 2, 8)) Then
ThisWorkbook.Sheets("Generators").Cells(i + 2, 8) = WorksheetFunction.
    VLookup(ThisWorkbook.Sheets("Generators").Cells(i + 2, 3),
    ThisWorkbook.Sheets("Generators").Range("M3:T6"), 7, False)
ThisWorkbook.Sheets("Generators").Cells(i + 2, 8).Font.Bold = True
ThisWorkbook.Sheets("Generators").Cells(i + 2, 7) = genenergy * 8000 / ((
    ThisWorkbook.Sheets("Generators").Cells(i + 2, 8) * 2 *
    WorksheetFunction.Pi / 60) ^ 2)
ThisWorkbook.Sheets("Generators").Cells(i + 2, 7).Font.Bold = True
End If
Next i

totenergy = ThisWorkbook.Sheets("Generators").Range("Q7").Value
TN = (totenergy / (freq0 ^ 2)) * 2 * freq0 * 0.98

End Function

Sub freqdyn()
Dim cof1 As Double, timestamp() As Double, timestamp2 As Double, t0 As Double,
    timestep As Double, timetot As Double, numtimesteps As Integer, i As Integer
Dim freq0 As Double, freq() As Double, freqi As Double, Pgen As Double, Pimb As
    Double, Pload As Double, kr As Double, Pload0 As Double
Dim numgen As Integer, tni As Double, freqrange() As Variant, n As Double, WS As
    Worksheet, sheetname As String
Dim numfreqs As Integer, Pshed As Double, Pgshed As Double, j As Integer,
    Pshedt0 As Double

' Obtain parameters
timestep = ThisWorkbook.Sheets("Parameters").Range("C9").Value / 1000
timetot = ThisWorkbook.Sheets("Parameters").Range("C10").Value
numtimesteps = timetot / timestep + 1
freq0 = ThisWorkbook.Sheets("UFLS").Range("B4").Value
freqi = freq0

```

```

numgen = ThisWorkbook.Sheets("Parameters").Range("C3").Value
numfreqs = ThisWorkbook.Sheets("Parameters").Range("C4").Value
n = ThisWorkbook.Sheets("Parameters").Range("C6").Value
If n = 0 Then
    n = 1#
End If
ReDim timestamp(1 To numtimesteps)
ReDim freq(0 To numtimesteps)
freq(0) = freqi
ReDim freqrange(0 To numfreqs, 5)

' Get the load
Pload = ThisWorkbook.Sheets("Parameters").Range("C5").Value
' Initial load self-regulation dependent on present Load but maintaining an
' initial frequency of 50 Hz
kr = Pload / freq0 * n
' Calculate T constant
tn1 = TN(numgen, freq0)
' Calculate total generation power
Pgen = 0
For i = 1 To numgen
    Pgen = Pgen + ThisWorkbook.Sheets("Generators").Cells(i + 2, 4)
Next i
' Calculate load, power mismatch and relay timer limit per each shedding
' frequency
For i = 0 To numfreqs
    ' Frequency thresholds
    freqrange(i, 1) = ThisWorkbook.Sheets("UFLS").Cells(i + 4, 2)
    Pshed = ThisWorkbook.Sheets("UFLS").Cells(i + 4, 3)
    ' Load power shedding
    freqrange(i, 2) = Pshed
    Pgshed = ThisWorkbook.Sheets("UFLS").Cells(i + 4, 4)
    ' Generation power shedding
    freqrange(i, 3) = Pgshed
    ' Relay timer count
    freqrange(i, 4) = 0
    ' Relay timer limit
    freqrange(i, 5) = ThisWorkbook.Sheets("UFLS").Cells(i + 4, 5) / timestep
Next i
'-----
' Prepare new Worksheet
Set WS = Sheets.Add
WS.Move After:=ActiveWorkbook.Sheets(ActiveWorkbook.Sheets.Count)
Cells(1, 1) = "Time"
Cells(1, 2) = "Freq"

```

```

Cells(1, 3) = "ROCOF"
Cells(1, 4) = "Pload"
Cells(1, 5) = "Pgen"
Cells(1, 6) = "Pimb"
Cells(1, 7) = "Pshed"

' Initiate values for main loop
cof1 = 0
Pshed = 0#
timestamp2 = 0#
Pimb = Pload - Pgen

' Main loop
For i = 1 To numtimesteps
    ' Determine current timestamp
    timestamp(i) = (i - 1) * timestep
    WS.Cells(i + 1, 1) = timestamp(i)
    ' Calculate new load-self regulation parameter.
    kr = Pload / freq0 * n
    ' Calculate new cof and new freq
    cof1 = COF2(Pimb, Pload, freqi, tnl, kr, timestamp2)
    freq(i) = freqi - cof1
    ' Apply load self-regulation using previous cof
    Pload = Pload - kr * (freq(i - 1) - freq(i))
    Pimb = Pload - Pgen
    ' Print main values used in this iteration
    WS.Cells(i + 1, 2) = freq(i)
    WS.Cells(i + 1, 3) = (freq(i - 1) - freq(i)) / timestep
    WS.Cells(i + 1, 4) = Pload
    WS.Cells(i + 1, 5) = Pgen
    WS.Cells(i + 1, 6) = Pimb
    WS.Cells(i + 1, 7) = Pshed
    Pshed = 0#
    ' New timestamp for next iteration
    timestamp2 = timestamp2 + timestep
    ' Determine Pload to be used for cof calculation of next iteration
    For j = 0 To numfreqs
        If freq(i) <= freqrange(j, 1) Then
            If freqrange(j, 4) = freqrange(j, 5) And cof1 >= 0 Then
                Pshed = Pshed + freqrange(j, 2)
                Pload = Pload - freqrange(j, 2)
                Pgen = Pgen - freqrange(j, 3)
                Pimb = Pload - Pgen
                timestamp2 = timestep
                freqi = freq(i)
            End If
        End If
    Next j
Next i

```

```

        End If
        freqrage(j, 4) = freqrage(j, 4) + 1
    End If
Next j
Next i

' Create basic scatter plot
WS.Shapes.AddChart2(240, xlXYScatterSmoothNoMarkers).Select
ActiveChart.SetSourceData Source:=Range(Range(Cells(1, 1), Cells(numtimesteps +
    1, 1)), Range(Cells(1, 2), Cells(numtimesteps + 1, 2)))

MsgBox "Done"

End Sub

```

Appendix B

Quality Report

The work was done during a five months internship in R&D NESTER. R&D NESTER is actively researching for better ways of grid operation. Considering the evolution of the grid towards a smarter and distributed network, the topic of having frequency operation ranges complying with European RfG codes at distribution level is very valid. The DSO may operate at other frequency ranges citing valid reasons such as avoiding uncontrolled islanding that may damage their equipment.

This issue was presented to R&D NESTER by the TSO, and R&D NESTER, along with ISEC, proposed this problem as a Master Thesis topic to the EMMC STEPS consortium. Once the project started, a literature review was done, mainly focusing on existing ENTSO-E papers, being that adherence to codes or authoritative recommendations was a priority. Afterwards, the work began, being based on actual topological information of the distribution network in Algarve back in December 2015, and the power flow information existing for those dates.

Daily communication existed with the company advisor, and constant periodic communication existed with the STEPS consortium advisor. There were no incidences during the work. No suggestion comes to mind when it comes to enhancing academic, administrative or technical issues. The experience was very gratifying, learned a great deal of academic topics and had an excellent professional experience. I strongly recommend to continue the partnership between R&D NESTER and the EMMC STEPS consortium, as it may greatly benefit both parties in the future.

Bibliography

- [1] EDP Distribuição. Caracterização das Redes de Distribuição a 31.Dez.2016. March 2017.
- [2] European Commission Regulation 2016/631. Network Code on Requirements for Grid Connection Applicable to all Generators (RfG). April 1983.
- [3] ENTSO-E. Dispersed generation report impact on CE region security. December 2014.
- [4] ENTSO-E. High Penetration of Power Electronic Interfaced Power Sources. March 2017.
- [5] IEEE Standard for Synchrophasor Measurements for Power Systems. *IEEE Std C37.118.1-2011 (Revision of IEEE Std C37.118-2005)*, pages 1–61, Dec 2011.
- [6] ENTSO-E. SPD DSA Task Force, Dynamic Security Assessment. May 2017.
- [7] T. van Cutsem and C. Vournas. *Voltage Stability of Electric Power Systems*. Kluwer international series in engineering and computer science. Springer, 1998.
- [8] ENTSO-E. Frequency Stability Evaluation Criteria for the Synchronous Zone of Continental Europe. March 2016.
- [9] ENTSO-E. Technical background for the Low Frequency Demand Disconnection requirements. November 2014.
- [10] EDP Distribuição. Plano de Desenvolvimento e Investimento da Rede de Distribuição 2015-2019.
- [11] Energias endógenas de Portugal. Available at <http://e2p.inegi.up.pt/>.
- [12] O. N. Faqhruldin, E. F. El-Saadany, and H. H. Zeineldin. Islanding detection for multi DG system using inverter based DGs. In *2013 IEEE Power Energy Society General Meeting*, pages 1–5, July 2013.
- [13] H. H. Zeineldin and J. L. Kirtley Jr. Performance of the OVP/UVP and OF-P/UFP Method With Voltage and Frequency Dependent Loads. *IEEE Transactions on Power Delivery*, 24(2):772–778, April 2009.

- [14] W. Freitas, Wilsun Xu, C. M. Affonso, and Zhenyu Huang. Comparative analysis between ROCOF and vector surge relays for distributed generation applications. *IEEE Transactions on Power Delivery*, 20(2):1315–1324, April 2005.
- [15] J. Cardenas, G. Mikhael, J. Kaminski, and I. Voloh. Islanding detection with Phasor Measurement Units. In *2014 67th Annual Conference for Protective Relay Engineers*, pages 229–241, March 2014.
- [16] Wikimedia Commons. File: Breadth-first-tree.svg — Wikimedia Commons, the free media repository, 2016. Available at <https://commons.wikimedia.org/w/index.php?title=File:Breadth-first-tree.svg&oldid=184866158>.
- [17] E. Žunić, A. Djedović, and B. Žunić. Software solution for optimal planning of sales persons work based on Depth-First Search and Breadth-First Search algorithms. In *2016 39th International Convention on Information and Communication Technology, Electronics and Microelectronics (MIPRO)*, pages 1248–1253, May 2016.
- [18] PowerWorld Corporation. Steady-State Power System Security Analysis with PowerWorld Simulator. S6: Voltage Stability Using PV Curves.
- [19] PowerWorld Corporation. Steady-State Power System Security Analysis with PowerWorld Simulator. S7: Voltage Stability Using QV Curves.
- [20] J. Aho, A. Buckspan, J. Laks, P. Fleming, Y. Jeong, F. Dunne, M. Churchfield, L. Pao, and K. Johnson. A tutorial of wind turbine control for supporting grid frequency through active power control. In *2012 American Control Conference (ACC)*, pages 3120–3131, June 2012.
- [21] UCTE. Final Report of the Investigation Committee on the 28 September 2003 Blackout in Italy. April 2004.
- [22] E. H. Camm, M. R. Behnke, O. Bolado, M. Bollen, M. Bradt, C. Brooks, W. Dilling, M. Edds, W. J. Hejidak, D. Houseman, S. Klein, F. Li, J. Li, P. Maibach, T. Nicolai, J. Patino, S. V. Pasupulati, N. Samaan, S. Saylors, T. Siebert, T. Smith, M. Starke, and R. Walling. Characteristics of wind turbine generators for wind power plants. In *2009 IEEE Power Energy Society General Meeting*, pages 1–5, July 2009.
- [23] E. Muljadi, V. Gevorgian, M. Singh, and S. Santoso. Understanding inertial and frequency response of wind power plants. In *2012 IEEE Power Electronics and Machines in Wind Applications*, pages 1–8, July 2012.
- [24] M. Fischer E. Quitmann, A. El-Deib, and S. Engelken. Anticipating Power System Needs in Response to the Global Energy Transition. In *CIGRE*, 2016.
- [25] N. W. Miller, K. Clark, and M. Shao. Frequency responsive wind plant controls: Impacts on grid performance. In *2011 IEEE Power and Energy Society General Meeting*, pages 1–8, July 2011.